NeuroImage 325 (2026) 121673

Contents lists available at ScienceDirect

NeuroImage

journal homepage: www.elsevier.com/locate/ynimg

Jumping to predictions: Auditory and visual prediction in hurdling

Sophie Siestrup [a,b,#,*], Marc Dührkop [a,b,#], Viviana Villafañe Barraza [a,1], Dennis Redlich [c], Alexandra Pizzera [c], Falko Mecklenbrauck [a,b], Jochen Bauer [d], Markus Raab [c], Ricarda I. Schubotz [a,b]

[a] Department of Psychology, University of Münster, Fliednerstraße 21, 48149 Münster, Germany
[b] Otto Creutzfeldt Center for Cognitive and Behavioral Neuroscience, University of Münster, Fliednerstraße 21, 48149 Münster, Germany
[c] Department of Performance Psychology, German Sport University Cologne, Am Sportpark Müngersdorf 6, 50933 Cologne, Germany
[d] Translational Research Radiology Imaging Center, Medical Faculty, University of Münster, Albert-Schweitzer-Campus 1, 48149 Münster, Germany

ARTICLE INFO

Keywords:
movement prediction
auditory
visual
fMRI

ABSTRACT

In everyday life, there are situations where sensory input can be temporarily unavailable. To maintain a coherent perceptual experience, the brain then relies on internal predictive models, shaped by prior experience and informed by sensory signals from different modalities such as audition and vision. The present study investigated how our brain actively compensates for brief masking of auditory and visual input at the example of hurdling, a complex full-body movement. Participants underwent functional magnetic resonance imaging (fMRI) while watching hurdling videos in which visual and/or auditory information was briefly masked, requiring the reliance on internal models during a movement prediction task. Between two fMRI sessions, participants completed six weeks of hurdling training to strengthen their own sensorimotor models of hurdling. As expected, prediction accuracy declined when sensory input was masked. Under visual masking, the brain not only relied more on the remaining auditory stream but also engaged frontal, motor, and visual regions despite the absence of visual input, hinting at top-down visual prediction. Auditory masks increased the recruiting of visual regions but showed no clear evidence for an auditory analogue of the top-down effect seen under visual masking. Predictive accuracy improved after hurdling training, and the training-related changes in neural activation overlapped with activation patterns under visual masking in frontal control and visuomotor areas, consistent with more efficient internal models for visual prediction. Due to field of view restrictions, no reliable effects could be detected in the cerebellar cortex. Taken together, we demonstrated that the brain flexibly recruited modality-specific networks depending on the available input and, in the case of missing visual information, predictions.

1. Introduction

In everyday life, we often need to control and perceive movements, even when sensory input is temporarily unavailable - for example, when we drive on the highway and a car briefly disappears behind a truck or when we talk to a friend and a loud noise briefly obscures their words. Whether as actors or as observers, we can still keep track of what is happening and anticipate what comes next, allowing us to respond appropriately. That is because, according to the predictive coding framework, the brain constantly predicts the most likely incoming sensory signals, based on internal predictive models (Clark, 2013). Predictions derived from these models travel down the neural hierarchy and are compared to actual sensory experiences. The difference between the two, the so-called prediction error, serves as a bottom-up learning signal to further improve predictive models and, in turn, allows us to optimize behavioral responses in the future. Taken together, in the exemplary situations described above, the brain relies on internal predictive models, shaped by prior experience and informed by sensory signals

* Corresponding author at: Sophie Siestrup, Department of Psychology, Fliednerstraße 21, 48149 Münster, Germany.
E-mail addresses: s.siestrup@uni-muenster.de (S. Siestrup), marc.duehrkop@uni-muenster.de (M. Dührkop), viviana.villafanebarraza@med.ovgu.de (V. Villafañe Barraza), d.redlich@dshs-koeln.de (D. Redlich), A.Pizzera@dshs-koeln.de (A. Pizzera), f_meck01@uni-muenster.de (F. Mecklenbrauck), jochen.bauer@uni-muenster.de (J. Bauer), Raab@dshs-koeln.de (M. Raab), rschubotz@uni-muenster.de (R.I. Schubotz).
Shared first authorship.
[1] Present address: Institute for Cognitive Neurology and Dementia Research, Otto-von-Guericke-University Magdeburg, Medical Faculty, Leipziger Str. 44, 39120 Magdeburg, Germany.

https://doi.org/10.1016/j.neuroimage.2025.121673
Received 29 September 2025; Received in revised form 18 December 2025; Accepted 19 December 2025
Available online 19 December 2025

from different modalities such as audition and vision, to infer unfolding events, including complex movements (Friston, 2005, 2012).

In the present study, we set out to investigate how predictive processes in different sensory modalities contribute to the perception and prediction of the same complex movement, namely hurdling. We chose hurdling because of the extreme importance of cadence here. While hurdlers do strongly rely on vision, making the visual modality the obvious candidate for prediction, hurdling also generates characteristic incidental movement sounds which are strongly rhythmic in nature, most so in expert hurdlers (MacPherson et al., 2009; Pizzera et al., 2017). In that sense, with increasing expertise, movement sounds produced during hurdling may become functionally similar to intentionally produced movement sounds, thereby becoming informative cues for prediction, too (Heins et al., 2020a; Murgia et al., 2017).

We employed a masking approach (auditory, visual, combined, or none) that allowed us to experimentally dissociate modality-specific prediction mechanisms. Our aims were threefold: first, to identify the neural networks that support auditory and visual predictions for complex whole-body movements; second, to determine the relative behavioral relevance of each modality; and third, to examine how predictive models themselves may change with practice.

As predictive models are thought to be shaped and refined through experience (Friston, 2005, 2012), we employed a pre-post training design in which participants practiced hurdling. This enabled us to investigate whether and how training modulates prediction-related brain networks as well as behavioral performance. Previous work has shown that both visual and auditory information are essential for predicting and controlling movements and that deprivation or distortion of either modality can impair performance (Schaffert et al., 2019; Senna et al., 2021; Shadmehr et al., 2010).

For the visual domain, continuous visual feedback provides essential information about movement direction, distance, and speed (Saunders & Knill, 2003, 2005). When visual input is transiently removed or occluded, perceptive performance decreases and predictive processes are enhanced to compensate for the missing information (Brich et al., 2018; Diersch et al., 2016; Stadler et al., 2011). Neuroimaging studies show that for these processes, biological-motion perception recruits occipito-temporal and fronto-parietal regions, including the middle-temporal area (MT), the fusiform gyrus, the dorsal premotor cortex (PMd), and the superior parietal lobe (SPL; Grosbas et al., 2012; Maes et al., 2020). For the auditory domain, natural movement sounds provide information about action quality and timing (Kennel et al., 2014, 2015; Müller et al., 2019; Schaffert et al., 2019). Distorted or delayed auditory feedback alters the perception of movements and modulates a hierarchical network comprising the primary auditory cortex, posterior superior temporal gyrus (pSTG), and supplementary motor area (SMA; Chennu et al., 2016; Heins et al., 2020a,b; Lima et al., 2016). Auditory deprivation can also elicit compensatory responses in this network, consistent with predictive coding accounts (Heins et al., 2020b; Pfordresher, 2006).

Taken together, these findings motivated us to test how predictive models operate during the perception of hurdling, a complex full-body movement. To this end, we implemented a hurdling-specific occlusion paradigm during fMRI sessions conducted before and after a training intervention in a pre–post design. In both sessions, participants observed point-light displays of a person hurdling in which visual and/or auditory information was transiently masked, requiring reliance on predictive models. To probe successful movement prediction, participants had the task to judge whether the speed of the hurdler had remained the same or changed throughout each video. Between sessions, participants completed six weeks of hurdle training. We hypothesized that such transient masking would (i) reduce accuracy in the movement prediction task and activity in primary sensory areas, (ii) differentially recruit modality-specific prediction networks (auditory: A1/pSTG/SMA; visual: MT/SPL/PMd), and (iii) that intensive motor training in hurdling would improve predictive accuracy and modulate these networks by strengthening internal models. We tested these hypotheses at the whole-brain level, as well as within these predefined regions of interest. The present study did not specifically test hypotheses about cerebellar involvement in the described processes, despite the relevance of this region in motor prediction (e.g., Nixon & Passingham, 2001; Ebner & Pasalar, 2008). This was due to the decision to choose a field of view that is optimal for investigating activation in (pre-)motor cortex, including SMA, and visual and auditory regions, which were the central areas of interest here. As a consequence, cerebellar activation could only be partially investigated, and the present study does not warrant strong conclusions about cerebellar mechanisms.

2. Materials and Methods

2.1. Participants

Eighty-six participants without prior hurdling experience, enrolled at German Sport University Cologne, attended the first scanning session of the present study. A complete dataset from two MRI sessions could only be obtained from 65 participants, as 21 participants had to be excluded for different reasons. Data from three participants could not be included due to technical problems during MRI acquisition, five participants self-reported low attentiveness during one of the scanning sessions and 13 participants terminated the study prematurely or did not complete the predefined required amount of training sessions (< 10), due to personal reasons. Please note that, as per our consent and data protection policy, participants were not required to state a reason why they wished to withdraw from the study, so that we cannot provide further details here. Furthermore, we did not exclude any participants due to their hurdling performance. The final sample of $N = 65$ included 27 men and 38 women, and participants' ages ranged from 19 to 29 years ($M = 22.62$, $SD = 2.27$). An a priori power analysis using G*Power (Erdfelder et al., 1996) with $\alpha = .05$, a power of .80 and an estimated effect size of .30 had predicted a required sample size of 66 participants. Most participants (58) were right-handed, as assessed by the Edinburgh Handedness Inventory (Oldfield, 1971). None of the participants reported any history of psychiatric or neurological disorder. All participants gave written informed consent to participate in this study and were monetarily reimbursed (296 €). The study was approved by the Local Ethics Committee of the University of Münster (Department of Psychology) as well as the Ethics Committee of the German Sport University Cologne in accordance with the Declaration of Helsinki.

2.2. Material

The presented stimuli were videos of a side-view point-light figure running over four hurdles using the common 3-step rhythm (4 contacts between hurdles). No hurdle, but only the figure was visible on the screen, staying fixated in the center to avoid saccadic eye as well as head movements by the participants in the scanner (Figure 1). Point-light displays were chosen for the present study to standardize the material and to be able to focus the participants' attention to the relevant details of the videos, that is, the rhythmicity of the movement. We have previously used such point-light displays in studies with the same focus (Heins et al., 2020a,b), and it is known that, despite their abstract nature, point-light videos are reliably perceived as biological motion by the brain (e.g., Saygin et al., 2004). The only sound audible in the videos was the hurdler's steps. The average video duration was 7.39 s (range: 5.88 to 9.0 s, SD = 0.93 s). To produce the stimuli, three athletes with different levels of hurdling experience (beginner, advanced, expert), assessed by licensed hurdle coaches from the German Sport University Cologne, were asked to run over four hurdles while being motion tracked and recorded. For motion tracking, we used the MVN Link Xsens motion capture suit and the software MVN 2022.0 (Schepers et al., 2018). The steps of the athletes were recorded with in-ear microphones. The trajectories and positions of the tracked data points of each athlete

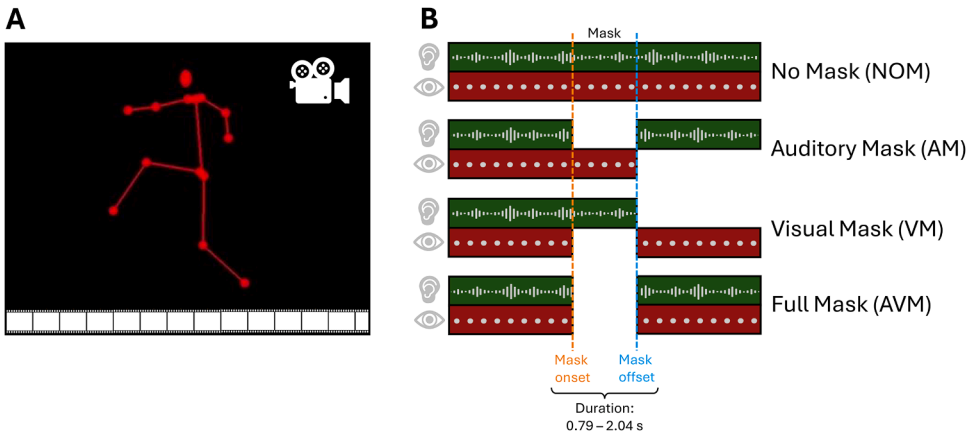

Figure 1. Overview of stimulus material.
Note. In the present study, we used videos showing a point-light figure running over hurdles for a movement prediction task (for task details, see Figure 2). Videos were derived from motion-tracked hurdle runs of real athletes and only showed the hurdler, fixed to the center of the screen, and included the sound of the hurdler's steps (A). While some videos were not manipulated (NOM), others included an auditory, visual, or full audio-visual mask (AM, VM, AVM, respectively) during which the respective sensory information was missing. Mask duration varied between 0.79 and 2.04 s (B).

were then exported and analyzed using MATLAB® version R2023a (The MathWorks, Inc.). We generated mute videos in which hurdlers were represented as point-light figures using the imported data in Psychtoolbox 3 (Kleiner et al., 2007). For synchronizing the recorded audio and mute videos obtained from MATLAB®, we used DaVinci Resolve® 18 (Blackmagic Design Pty. Ltd., South Melbourne, Australia). To enable a later analysis of missing visual and/or auditory information, different versions of the videos were created in which some sensory information was removed. We refer to these manipulations as masks in the following. Three types of masks were used: auditory masks (AM), in which the hurdler could be seen but not heard; visual masks (VM), in which the hurdler could be heard but not seen; and full audio-visual masks, in which the hurdler could be neither seen nor heard (AVM). Masks started immediately after the launching step for transversion of the second hurdle (we refer to this timepoint as mask onset in the following) and covered two, three, or four steps and ended immediately before the following step (which was an intermediate, launching, or landing step, respectively; we refer to this timepoint as mask offset in the following). We chose this timepoint for mask onset to ensure that enough (clearly rhythmic) information was presented before the masking to facilitate the establishment of a predictive model of the rhythm on a trial-by-trial basis. Mask duration varied between 0.79 and 2.04 s. Together with the differences in video duration (see above) this variability provided a natural jittering of the task, which is beneficial for the efficiency of an event-related fMRI design. Importantly, after the mask offset when the previously masked sensory modality returned, the other respective modality was masked until the end of the video. In the case of the AVM, both modalities returned (Figure 1). This mask switch was implemented so that participants could not simply rely on the remaining sensory input alone but would have to rely on their internal movement model to be able to predict the course of the action. We used videos with no mask (NOM) as a control condition. Additionally, to assess general effects of perceiving meaningful hurdling movements, we created another type of control stimulus, so-called scrambled videos (SCB). To this end, we cut each of the original videos into 125 ms segments and randomly reassembled those parts using DaVinci Resolve® 18.

Variations in hurdler expertise (beginner, advanced, experts) and mask duration (2, 3, 4 steps) were introduced to increase variability in the stimulus material and thus give rise to more robust results. All of these factors were perfectly balanced for each participant and will not be further analyzed in the present paper.

To assess how well participants could rely on their internal movement model in the different conditions, we designed a task that required them to tune into the beat of the hurdling movement and use top-down predictions to answer correctly (see section 2.3.2.1 for a detailed description of the task). From intense behavioral piloting, we identified a speed detection task as the most suitable task of appropriate difficulty that, at the same time, allowed for accounting for natural variability in the stimulus material. To this end, we applied a speed manipulation to 50% of the videos using DaVinci Resolve® 18. The beginner and advanced hurdler speeds were modified to 80% and 125% of their original speed, respectively. The speed of the expert hurdler was modified to 75% and 110% of the original speed. These particular manipulations were chosen to induce noticeable changes in speed, but at the same time avoid making the movement appear unnaturally fast or slow, as validated by the experimenters. Importantly, the speed manipulation only affected the time between the mask offset and the end of the video. For NOM and SCB videos where no mask was implemented, we used the corresponding timepoints of the masked videos as reference points for the speed manipulation.

2.3. Procedure

The present study was part of a large cooperation project with the German Sport University Cologne to address several different research questions. Therefore, the study design was relatively complex and not all findings are reported in the present paper. For more clarity, we also provide some methodological details in the Supplementary Material only.

The study consisted of three parts. For the first part, participants engaged in the first MRI session at the University of Münster. During this session, they underwent an fMRI measurement during which they were presented with the above-described point-light video stimuli to assess brain responses during different masking conditions. In parallel, participants completed a movement prediction task to assess how well they could rely on their internal predictive model of hurdling in the different conditions (see section 2.3.2.1). Additionally, we acquired several structural measures of the brain (standard anatomical T1 images, Diffusion Tensor Imaging; DTI, quantitative MRI; qMRI; see section 2.3.2.2 and Supplementary Material) to investigate how intense physical training influences structural brain organization. The results of structural analyses are not reported here but in a companion paper (Dührkop et al., in preparation).

In the second part of the study, participants attended a six-week hurdling training program at the German Sport University Cologne. To investigate how incidentally generated movement sounds affect motor learning, participants were divided into three different training groups (normal feedback, $N = 21$; auditory focus, $N = 23$; and auditory

deprivation, $N = 21$; see section 2.3.1). Behavioral results of the hurdling training under varying auditory feedback conditions will be reported in a companion paper (Redlich et al., under review), as the present paper focuses on the neurofunctional findings. Importantly, due to the equal distribution of participants to the different training groups, we can rule out a systematic confound thereof on the data reported here. The controlled variability of training experiences might have even positively influenced the robustness of the effects presented in the present paper.

In part three, participants underwent a second MRI session that followed the same protocol as described above for part one. The aim of the second fMRI measurement was to examine the effect of motor training on the perception and prediction of hurdle running and respective neurofunctional and behavioral correlates thereof, given the strengthening of the internal predictive movement model of hurdling.

2.3.1. Hurdle Training

In the following, we provide a brief overview of the hurdle training procedure. For more details, see Supplementary Material.

The training was based on the usual requirements of the teaching plans for sport students' hurdle training as well as the basic training plan by the German Athletics Association and was conducted by licensed coaches. As mentioned above, we split the participants into three training groups to investigate the effect the deprivation of and focus on incidentally generated movement sounds exhibit on motor learning. Please note that the different groups are not of interest for the current paper and will therefore be further described in a companion paper (Redlich et al., under review). All groups participated in a total of 10 - 12 hurdling training sessions over six consecutive weeks (twice-weekly, equivalent to the usual training volume in beginner athletics courses). Hurdle training included three difficulty levels (t1, t2, and t3) with varying distances between the hurdles and increased height of the hurdles in t3. We implemented a pre-test (week one), two intermediate tests (week four and week six), a post-test (week seven), and a retention test (week 10, after the second MRI session) to track the development of participants' performance over the training. The participants' individual hurdling performance as well as specific improvements therein are analyzed in detail in the companion paper (Redlich et al., under review).

2.3.2. fMRI Sessions

2.3.2.1. Task. Immediately before entering the scanner, participants completed a short training on a laptop to familiarize themselves with the stimulus material as well as the prediction task. The training comprised three blocks. During the first block, participants were presented the point-light videos of the three hurdlers once each. They were instructed to watch the videos attentively, but no behavioral response was required. Next, 18 videos of the different mask conditions (AM, VM, AVM) were presented, followed by a block of 9 SCB videos. During blocks two and three, participants performed the same task as later in the scanner. They were instructed to attentively watch the video and judge whether the runner maintained the same speed throughout the video (50% of the videos) or not (25% faster, 25% slower) by pressing two different buttons on the keyboard. They were made aware of the fact that the speed change would occur after mask offset. During training only, participants received immediate feedback (500 ms) whether they had responded correctly, incorrectly, or too late (i.e., more than 500 ms after the video had ended). The order of videos within blocks was randomized for each participant. Importantly, if participants reached less than 60% correct responses, the training was repeated once. One training session lasted for about 5.5 min.

After entering the scanner, participants were first presented with a sample of the hurdling sounds while an echo planar imaging (EPI) sequence was running and could adjust the volume of the recording individually to make sure the scanner noise would not drown out the auditory stimuli.

During the following fMRI measurement, participants were presented with the above-described stimuli. In total, participants had to complete 186 trials, divided into six blocks. In each block, only stimuli from one runner (beginner, advanced, expert) were presented, resulting in each runner being presented in two blocks. Each block consisted of six NOM videos, 18 videos with a mask (six each for AM, VM, and AVM), four SCB videos, and three null events (fixation cross on a grey background for 7 s). In total, there were 36 trials for the NOM, AM, VM, and AVM conditions, 24 for SCB, and 18 null events. Block order was balanced over participants. Half of the videos per block were presented at normal speed, while the other half were either sped up or slowed down, as described above. The videos were presented in a pseudo-random order so that the same experimental condition could be repeated maximally four times in a row, and there were always at least five video trials between two null events. For all trial types except for null events, an interstimulus interval of 2.5 s, during which a fixation cross was presented, was used. In the case of null events, the fixation cross was instead presented for 7 s. Furthermore, video trials ended with 500 ms of fixation cross as an extension of the response window for participants.

During each video, participants were required to judge whether the runner shown in the video changed or maintained their speed, as described above. This task was used because it requires the participants to tune into the beat of the hurdling rhythm and maintain it also during the masked parts using top-down predictions. For responding, participants used two buttons on a four-button response box. They were instructed to press the left button with their index finger if they perceived the hurdler's speed to remain the same and press the right button with their middle finger if they believed the speed was manipulated (slowed down or sped up). No feedback was provided during the completion of the task in the scanner. The whole duration of one task session was around 30 minutes. Figure 2 shows an example trial of the prediction task used during the scanner sessions.

2.3.2.2. MRI Acquisition. Participants were scanned in a 3-Tesla Siemens Magnetom Prisma MR tomograph (Siemens, Erlangen, Germany) using a 20-channel head coil. A 3D multiplanar rapidly acquired gradient-echo (MPRAGE) sequence was used to obtain high-resolution T1-weighted images ahead of functional scanning, with scanning parameters set to 192 slices, a repetition time (TR) of 2130 ms, an echo time (TE) of 2.28 ms, a slice thickness of 1 mm, a field of view (FoV) of 256×256 mm^2, and a flip angle of 8°.

Gradient-echo echoplanar imaging (EPI) was used to measure the blood-oxygen-level-dependent (BOLD) contrast for functional imaging data of the whole brain. Scanning parameters were set to a TE of 30 ms, a TR of 1500 ms, a flip angle of 71°, 63 slices with a slice thickness of 2.4 mm (voxel size: $2.5 \times 2.5 \times 2.4$ mm^3), an acceleration factor of 3, and a FoV of 210×210 mm^2 (please note that approximately the lower half of the cerebellum could not be included in the FoV). For later correction for magnetic field inhomogeneities, we additionally acquired five images with an EPI sequence that was equivalent to the one reported above, but with a 180° flip along the y-axis (we refer to this as inverted EPI sequence in the following). Furthermore, we acquired diffusion-weighted imaging as well as qMRI (Guilfoyle et al., 2003) sequences. Because the results of these additional MRI acquisitions are not reported in the present paper, the corresponding scanning parameters are provided in the Supplementary Material.

2.4. Statistical Analysis

2.4.1. Individual Improvement in Hurdling Performance

For understanding the establishment and consolidation of a predictive movement model of hurdling in the brain, the individual training success might play an important role. While the participants' individual

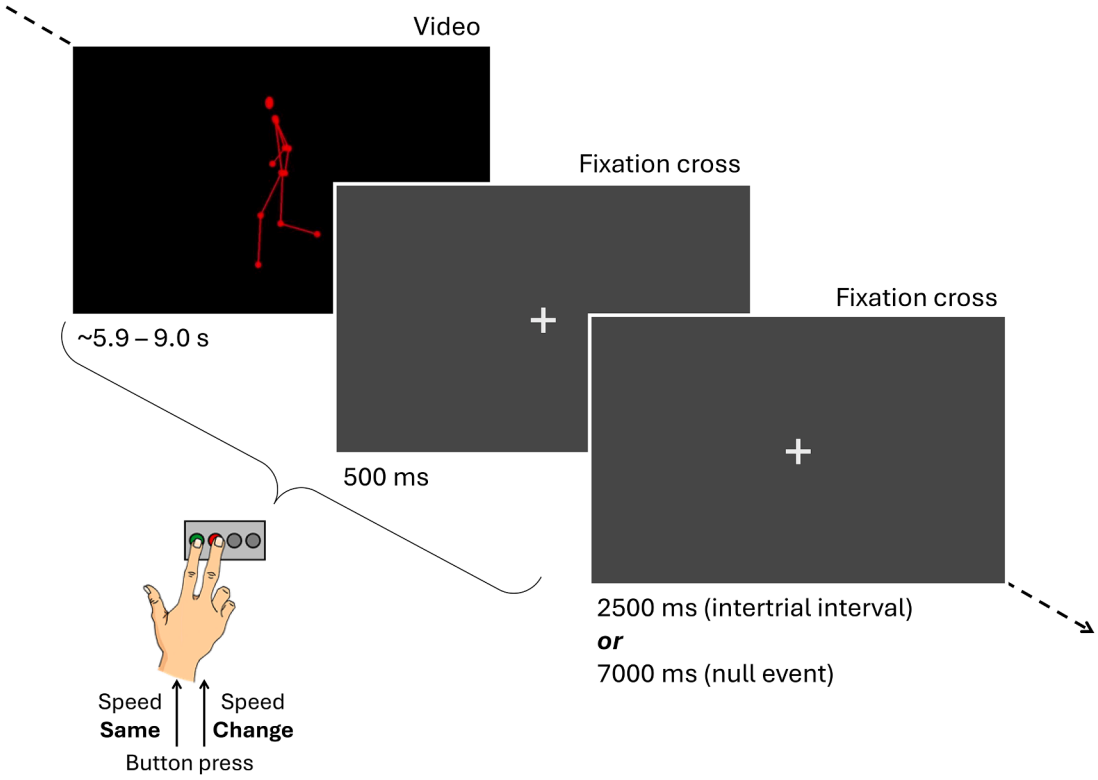

Figure 2. Example trial of the movement prediction task.
Note. Each video trial of 5.9 – 9.0 s was embedded by a 2.5 s intertrial interval during which a fixation cross was presented. In the case of null events, the fixation cross was displayed for 7 s. Additionally, 500 ms of fixation cross were added after each video as an extension of the response window. After mask offset, the video speed either remained the same or changed, and the participants' task was to indicate this with a button press. Participants were supposed to press the left button with their index finder when the hurdler's speed remained the same and press the right button with their middle finger when the speed was manipulated.

hurdling improvements are presented in detail in the companion paper (Redlich et al., under review), we still considered this an important influencing factor for the present analyses. For this reason, we calculated individual hurdling improvement (most improved athlete, MIA) scores from before to after the training to include as a covariate in our analyses.

First, we calculated the so-called technique index (TI) before and after the training period for each participant, using the data acquired during the pre- and the post-test. The TI was defined as the ratio of the time it took to run over the hurdle course and sprinting the same distance (Kaisidou et al., 2021). A separate TI was calculated for the t1 and t2 training difficulties and then averaged for each timepoint. Note that for the t3 difficulty, no TI was calculated, as eleven participants did not master the hurdling course at this difficulty stage, even after intense training. Finally, MIA was defined as the difference between the average TI after and before the training period.

Due to technical difficulties during hurdling recordings, no TI was available for 6 participants at one or both timepoints. To avoid an exclusion of these participants from fMRI analyses, missing TI datapoints were interpolated using the k-Nearest Neighbor Imputation of the VIM package (Kowarik & Templ, 2016) in RStudio (R Core Team, 2025; Version 2025.05.0) to then calculate MIA scores.

2.4.2. *Behavioral Data Analysis*

To assess whether the different masking conditions affect how well participants can predict movements based on their internal model, we analyzed the mean accuracy and reaction times (RT) per condition and timepoint from the prediction task. The analysis of behavioral data was conducted with RStudio (R Core Team, 2025; Version 2025.05.0).

For the analysis of accuracy, missed and preliminary responses (i.e., before mask offset when the speed manipulation became detectable, which means, outside of the valid response window) were counted as correct in 50% (chance level) of the cases. By doing so, we followed the recommendation to not count missing responses as incorrect in the analysis of accuracy (e.g., De Ayala et al., 2001), but to treat them as fractionally correct (Dai, 2021).

For the analysis of RTs, only truly correct responses were considered. Extreme outliers per condition and participant (as defined as values above 3rd quartile + 3 * interquartile range (IQR) or lower than 1st quartile – 3 * IQR) were excluded for the RT analysis on a single-trial basis prior to forming averages per condition. One participant was excluded from the RT analysis completely, as they did not produce any correct responses in one condition (SCB).

For the statistical analysis, we used repeated measures ANOVAs (rmANOVAs) with the factors Time (pre, post) and Condition (NOM, AM, VM, AVM, SCB) and the covariates Gender and MIA (mean-centered). By using a repeated-measures design, we ensured that the individual differences between subjects were accounted for in the analysis. As post-hoc tests, we applied paired *t*-tests (one- or two-sided, depending on hypothesis), corrected for multiple comparisons with Bonferroni-correction. Additionally, we performed an exploratory post-hoc test for the Time x Condition interaction. For this, we calculated the pre-to-post increase in accuracy and decrease in RT per condition and used an rmANOVA with the factor Condition. Additionally, we applied one-sided one-sample *t*-tests against zero for each condition to test for significant increases/decreases of the described variables individually to better understand the influence of the hurdling intervention on the hypothesized performance improvement for the different masking conditions. *P*-values obtained from these one-sample *t*-tests were adjusted for multiple comparisons using Bonferroni-correction, and are reported accordingly.

Lastly, we performed a control analysis to investigate whether improvements in the movement prediction task would be expected from

task familiarization alone. To this end, we performed a rmANOVA with the factor Block (with six levels) on accuracy and RT data from the first fMRI session.

We report mean values and standard errors of the mean. A significance level of $\alpha = .05$ was applied. Normality was assessed using the Shapiro-Wilk test. Whenever the assumption of sphericity was violated (Mauchly's test of sphericity), we report Greenhouse-Geisser-corrected degrees of freedom and *p*-values.

2.4.3. fMRI Data Analysis

2.4.3.1. Preprocessing. The MRI images were processed using SPM12 (Wellcome Trust, London, England) and FSL (Jenkinson, 2012; Smith et al., 2004; version 6.0.5). First, fMRI images were corrected for B_0 field inhomogeneities using the *topup* and *applytopup* (Andersson et al., 2003; Smith et al., 2004) functions in FSL. For the fieldmap estimation in *topup*, we used the last three images of the EPI and inverted EPI sequences.

The remaining preprocessing of functional data was conducted in SPM12, including slice time correction to the first slice, movement correction and realignment to the mean image, co-registration of each participant's anatomical scan to the mean functional image, normalization into the standard MNI (Montreal Neurological Institute, Montreal, QC, Canada) space based on segmentation parameters including resampling of the functional images to 2.5 mm^3, and spatial smoothing using a Gaussian Kernel full-width half maximum (FWHM) of 8 mm. A 128-s high-pass temporal filter was applied.

2.4.3.2. fMRI Model Specification. fMRI data were analyzed in SPM12 using general linear models (GLMs) for serially autocorrelated observations (Friston et al., 1994; Worsley & Friston, 1995). For each participant, we used the smoothed (8-mm FWHM) normalized gray matter image obtained from segmentation, which was thresholded at .2 using ImCalc in SPM12, to create a binary gray matter mask that was applied at the first level of analyses.

On the first-level, we calculated two GLMs (GLM1, GLM2) on fMRI data from before and after the training phase (Pre, Post):

GLM1 focused on the neural correlates of the different masking conditions and included 19 regressors. For each type of (masking) condition (NOM, VM, VM, AVM, SCB), we added two regressors, modelled as events due to their brief duration. Onsets were time-locked to the points of mask onset to model brain responses during the short (0.79 to 2.04 s) mask interval. Additionally, we modeled the event of mask offset as a proxy of participants' responses, as at this time-point, a button press was required from them. We validated that the time-point of mask offset well represented this motor response by inspecting the mask offset > null event contrast for the expected activation in sensory motor areas. For NOM and SCB trials, the hypothetical times of mask onset and offset were used, as derived from the masked video counterparts. Furthermore, we added two more regressors for the full duration of NOM and SCB trials as additional controls (fullNOM, fullSCB), with onsets time-locked to the beginning of the video. Null events were modeled with their full presentation time (7 s), as this duration provided a long enough time window for the meaningful modeling as epochs. Regressors were convolved with the canonical hemodynamic response function. Additionally, the six subject-specific rigid-body transformations obtained from realignment were included as regressors of no interest.

GLM2 focused on the relation of functional data to behavioral performance in the prediction task. We reasoned that when participants are able to successfully draw information from their predictive model to identify speed changes, we should specifically see evidence of brain activation in modality-specific predictive networks. The model specifications were as described above for GLM1, but the regressors coding for the mask onsets of AM and VM were split into correct and incorrect responses ($AM_{correct}$, $AM_{incorrect}$, $VM_{correct}$, $VM_{incorrect}$). Only truly correct responses were included in the $AM_{correct}$ and $VM_{correct}$ regressors (i.e., no missed or preliminary responses, which were included in the $AM_{incorrect}$ and $VM_{incorrect}$ regressors) to be able to pinpoint neural activation related to successful prediction only. To ensure meaningful statistical modeling of brain responses, each regressor had to include at least 5 trials, which led to the exclusion of 13 participants from this particular analysis. The number of trials per regressor ranged from 5 to 31 per participant ($M = 18$). Please note that due to this reduced number of participants and trials per regressor, as well as the partially uneven distribution of trial numbers, the sensitivity of this second GLM was likely compromised.

2.4.3.3. Whole Brain Analysis. For GLM1, we calculated the first-level contrasts VM>NOM (reflecting a situation where no visual but only auditory input is available), VM>AVM (reflecting an isolated focus on the auditory modality), AM>NOM (reflecting a situation where no auditory but only visual input is available), AM>AVM (reflecting an isolated focus on the visual modality), and NOM>SCB (reflecting brain activation for the general perception of natural hurdling movements). Additionally, we calculated the reverse contrasts NOM>VM and NOM>AM to investigate the hypothesized downregulation in auditory and visual cortices in the absence of the respective stimulus. For GLM2 the contrasts $AM_{correct}$>$AM_{incorrect}$ as well as $VM_{correct}$>$VM_{incorrect}$ were calculated. For all contrasts, we used the condition regressors based on the mask onsets.

For second-level group analyses, we applied a full-factorial design with Time as a factor and Gender and MIA (mean-centered) as covariates. For each first-level contrast of GLM1 and GLM2, we calculated the positive effect of condition (*t*-contrast), i.e., the overall condition effect, and the main effect of Time (*F*-contrast). When the latter showed significant activation after correction (see below), we additionally calculated the Pre>Post and Post>Pre *t*-contrasts. We applied false discovery rate (FDR) correction and used a minimal threshold of $p < .05$ (voxel level) to determine significant activation. FDR correction provides greater sensitivity for detecting effects than more conservative methods, such as family-wise error correction (Genovese et al., 2002; Poldrack et al., 2011). We therefore chose FDR for this first-of-its-kind study to reduce the risk of overlooking meaningful activations in hypothesized regions. Since we often found very large activation clusters spanning multiple brain regions with this minimal significance threshold, but at the same time wanted to apply the same correction method (FDR) to all T-maps, we report several T-maps with a higher threshold of $p < .0001$ for a more comprehensible report. Generally, we only report clusters with a minimum size of 20 voxels. Brain activation was visualized with MRIcroGL (Version 1.2.20220720 × 86-64 FPC, McCausland Center for Brain Imaging, University of South Carolina).

2.4.3.4. ROI Analysis. To specifically investigate brain responses in hypothesized regions, we performed a planned region of interest (ROI) analysis in predefined brain regions belonging to the auditory and visual processing and prediction networks.

Functional ROIs were constructed as spheres with a radius of 8 mm around previously published peak voxel coordinates in MNI space, using the MarsBar Toolbox (Brett et al., 2002). ROIs were left and right A1 (x = -42, y = -22, z = 7; x = 46, y = -14, z = 8; Jo et al., 2019), pSTG (x = -61, y = -32, z = 8; x = 59, y = -25, z = 8; Jo et al., 2019), SMA (x = 10, y = 4, z = 54; x = -6, y = 4, z = 54; Jo et al., 2019), V1 (x = -12, y = -88, z = 2; x = 12, y = -88, z = 2; Kuhnke et al., 2023), MT (x = -44, y = -76, z = 4; x = 46, y = -70, z = 0; Kuhnke et al., 2023), PMd (x = -32, y = -4, z = 52; x = 26, y = 0, z = 56; Kuhnke et al., 2023), and SPL (x = -20, y = -64, z = 58; x = 22, y = -62, z = 56; Kuhnke et al., 2023). Please note that coordinates used for SMA and V1 were manually adjusted for better symmetry across hemispheres. Beta values were extracted from the first-level contrasts VM>NOM, VM>AVM, AM>NOM, AM>AVM, and

NOM>SCB and averaged over hemispheres.

To analyze the extracted beta values, we first tested for general activation/deactivation within each ROI. To this end, we applied one-sample *t*-tests against zero with regard to our hypotheses. Within each ROI, we used Bonferroni-correction to correct for multiple testing and report the corrected *p*-values. To then analyze the influence of hurdling training on brain activation, we used rmANOVAs with the factor Time (Pre, Post) and the covariates Gender and MIA (mean-centered) in RStudio (R Core Team, 2025; Version 2025.05.0). Additionally, when significant (interaction) effects for MIA were found, we further investigated the relationship of MIA with beta values using exploratory Pearson correlations. Reported *p*-values were corrected for multiple comparisons using Bonferroni-correction. Additionally, we used exploratory Pearson correlations to further assess the connection between behavioral accuracy in the VM, AM, and NOM conditions with betas extracted from A1, V1, and SMA (a region high in the predictive hierarchy) from the VM>NOM and AM>NOM contrasts. *P*-values were corrected for multiple comparisons. However, we could not detect any significant correlations here (all $p > .57$).

We report mean values and standard errors of the mean. A significance level of $\alpha = .05$ was applied.

3. Results

3.1. Behavioral Results

To assess the behavioral costs of omitted sensory input during hurdling prediction, we analyzed the mean accuracy and reaction times (RT) per condition and timepoint from the fMRI task (Figure 3).

For accuracy, we found a significant main effect of the factor Time ($F(1, 62) = 13.84$, $p < .001$, $\eta_p^2 = .182$), meaning participants' performance improved after hurdling training, as expected. Additionally, there was a significant main effect of Condition ($F(2.54, 157.31) = 79.70$, $p < .001$, $\eta_p^2 = .563$). Paired *t*-tests revealed that accuracy in the NOM

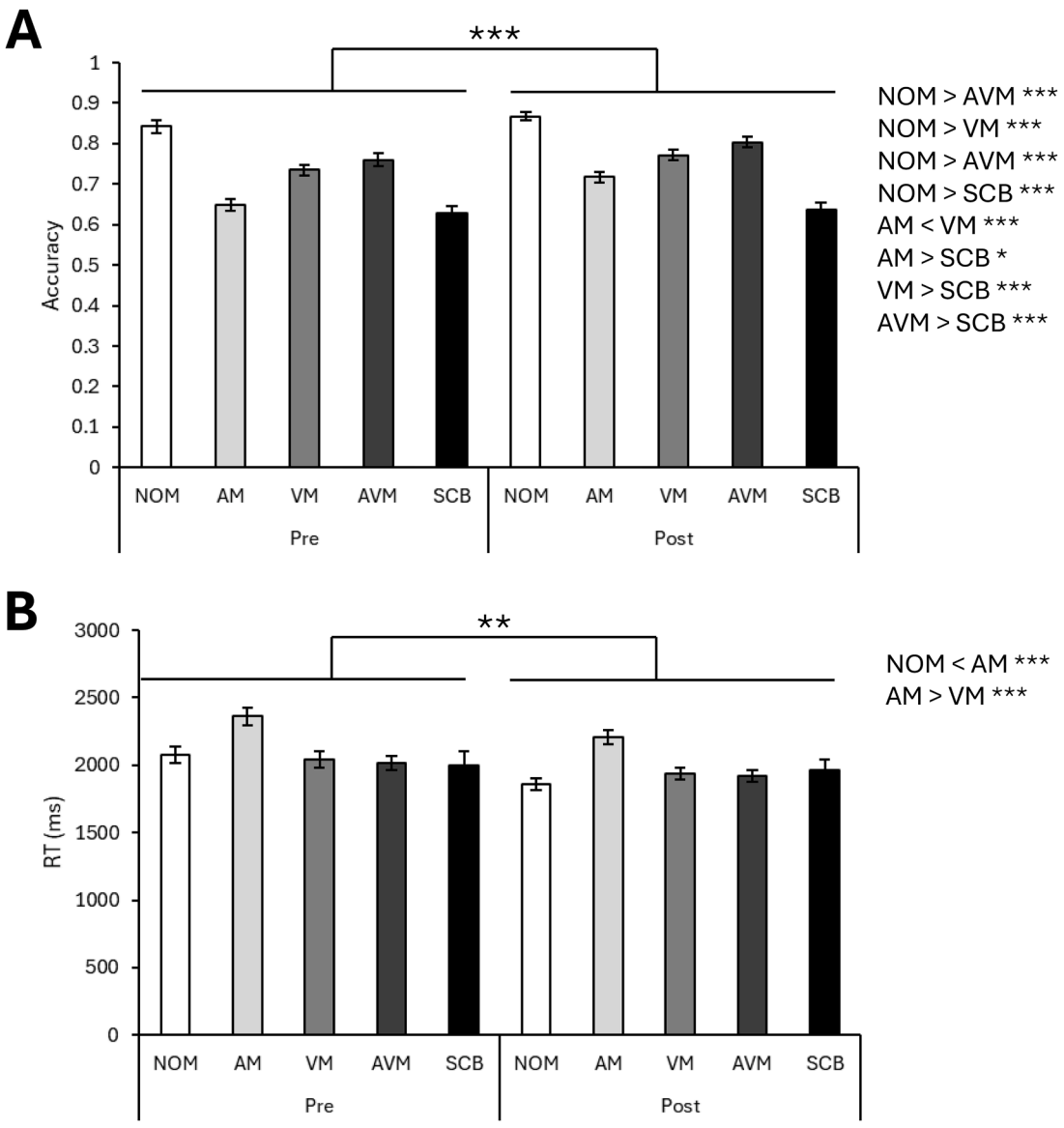

Figure 3. Behavioral results from movement prediction task during fMRI sessions.
Note. During two fMRI sessions, one before (Pre) and after (Post) hurdling training, participants watched videos of a point-light hurdler. In some videos, auditory information (AM), visual information (VM) or both (AVM) were missing for a brief duration. Some videos were presented without any missing sensory information (NOM), and some were edited into random, scrambled sequences (SCB). The participants' task was to tune into the beat of the hurdling movement and decide whether the speed remained the same throughout each video. We analyzed accuracy (A) and RT (B) as performance measures. Statistics: rmANOVAs and post-hoc paired *t*-tests. * = $p < .05$, ** = $p < .01$, *** = $p < .001$.

condition was higher than in the AM ($t(64) = 15.16$, $p < .001$, $d = 1.88$), VM ($t(64) = 11.12$, $p < .001$, $d = 1.38$), AVM ($t(64) = 7.82$, $p < .001$, $d = 0.97$), and SCB ($t(64) = 12.45$, $p < .001$, $d = 1.54$) conditions. Additionally, accuracy in the SCB was also significantly lower than in the AM ($t(64) = 3.05$, $p = .017$, $d = 0.38$), VM ($t(64) = 7.43$, $p < .001$, $d = 0.92$), and AVM ($t(64) = 8.85$, $p < .001$, $d = 1.10$) conditions. Interestingly, we also found that accuracy in the AM condition was significantly lower than in the VM condition ($t(64) = -5.54$, $p < .001$, $d = -0.69$). There was also a significant effect of the covariate Gender, as men showed a higher mean accuracy compared to women ($M_{men} = .768 \pm .013$, $M_{women} = .721 \pm .010$; $F(1, 62) = 9.75$, $p = .003$, $\eta_p^2 = .136$). We did not find further significant main or interaction effects (all $p > .05$, $\eta_p^2 < .035$), but opted for an exploratory post-hoc analysis for the Time x Condition interaction due to a non-significant trend detected here ($F(2.75, 170.53) = 2.21$, $p = .094$, $\eta_p^2 = .034$). For this, we calculated the pre-to-post training increase in accuracy per condition. A near-significant trend for an effect of Condition ($F(2.75, 170.53) = 2.21$, $p = .094$, $\eta_p^2 = .034$), but no further significant main or interaction effects could be detected ($p > .05$, $\eta_p^2 < .01$). One-sample *t*-tests against zero were used to further investigate the condition-wise improvement as hinted at by the statistical trend for a Condition effect. These revealed significant improvement from before to after the hurdling training only in the AM ($t(64) = 4.09$, $p < .001$, $d = 0.508$), VM ($t(64) = 2.74$, $p = .019$, $d = 0.340$), and AVM ($t(64) = 2.67$, $p = .023$, $d = 0.331$) conditions, but not in the NOM ($t(64) = 1.67$, $p = .252$, $d = 0.207$) and SCB ($t(64) = 0.36$, $p = 1$, $d = 0.045$) conditions.

Regarding RT, there was a significant main effect of Time ($F(1, 61) = 10.88$, $p = .002$, $\eta_p^2 = .151$), as participants became faster to respond correctly after training. Additionally, we detected a significant main effect of Condition ($F(1.91, 116.25) = 18.08$, $p < .001$, $\eta_p^2 = .229$). Paired *t*-tests revealed that participants answered significantly faster in the NOM ($t(63) = -11.13$, $p < .001$, $d = -1.39$) and VM conditions ($t(63) = 7.70$, $p < .001$, $d = 0.96$) compared to the AM condition. We did not find further significant main or interaction effects ($p > .05$, $\eta_p^2 < .045$), but again a non-significant trend for a Time x Condition interaction ($F(2.26, 138.03) = 2.83$, $p = .056$, $\eta_p^2 = .044$). An exploratory post-hoc analysis on condition-wise RT decreases revealed a non-significant trend for a Condition effect ($F(2.26, 138.03) =$, $p = .056$, $\eta_p^2 = .044$). One-sample *t*-tests against zero were applied to further investigate the condition-wise improvement in RTs. These demonstrated significant RT decreases for the NOM ($t(63) = 4.91$, $p < .001$, $d = 0.614$), AM ($t(63) = 2.77$, $p < .001$, $d = 0.346$), VM ($t(63) = 2.89$, $p = .013$, $d = 0.361$), and AVM ($t(63) = 2.85$, $p = .015$, $d = 0.357$) conditions, but not for the SCB condition ($t(63) = 0.49$, $p = 1$, $d = 0.06$).

The control analysis to investigate possible task improvement due to familiarization effects revealed no significant improvement over the course of the first fMRI session for accuracy ($F(3.99, 255.42) = 0.77$, $p = .542$, $\eta p2 = .012$) or RT ($F(3.94, 251.95) = 2.27$, $p = .063$, $\eta p2 = .034$).

3.2. Whole Brain Results

To test our hypothesis that a transient masking of one sensory modality would reduce activity in respective primary sensory areas, we contrasted the NOM condition with the individual mask conditions (AM, VM). The whole brain contrast NOM>AM from GLM1 yielded higher activation in left and right Heschl's gyrus. Accordingly, the contrast NOM>VM revealed higher activation in the right visual cortex (V1).

Next, we investigated whether transient masking of auditory and/or visual information recruits modality-specific prediction networks. In the VM>NOM contrast, reflecting a situation where no visual but only auditory input is available, we found higher brain activity in Heschl's gyrus, pSTG, supramarginal gyrus (SMG), the SMA, the precuneus, Area MT, and V1. Additionally, the VM>AVM contrast, representing an isolated focus on the auditory modality, revealed higher activation in Heschl's gyrus, the precentral gyrus (BA 4), and pSTG.

The AM>NOM contrast, reflecting available visual but no auditory input, showed increased activity in the amygdala as well as V1, the fusiform gyrus, area MT, the PMd, the SPL, and cerebellum. The AM>AVM contrast, i.e., a specific focus on visual input, revealed higher activation in the posterior cingulate gyrus, fusiform gyrus, primary visual cortex, area MT, cerebellum, and the intraparietal sulcus (IPS).

To see which brain areas are involved for the general perception of natural hurdling movements, we additionally calculated the NOM>SCB contrast. Here, we observed increased activity in the superior frontal gyrus (SFG), V1, inferior frontal gyrus, angular gyrus, and the pCC.

Regarding the pre- vs. post-training comparison, only the NOM>SCB and VM>NOM contrasts revealed significant differences before and after the hurdle training. In the NOM>SCB contrast, the mPFC, the angular gyrus, the middle temporal gyrus, parts of the cuneus and precuneus, and cerebellum, were more active in the first MRI session. For the VM>NOM contrast, we found more activity in the first MRI session in the anterior insula, the SMA, the middle frontal gyrus, and the left superior frontal gyrus. Peak activity coordinates (Table 1 and Table 2) and visualizations of the results of GLM1 (Figure 4 and Figure 5) can be found below.

Additionally, we calculated a second GLM to investigate the relation of functional data and behavioral performance in the prediction task. To this end, we formed contrasts between activation in trials with correct and incorrect responses in the mask conditions. These contrasts from GLM2 did not show any significantly activated brain regions after correction for multiple comparisons. However, for the $AM_{correct}>AM_{incorrect}$ contrast, we found subthreshold ($p < .05$, uncorrected) activation in several hypothesized brain regions, including primary and secondary auditory cortices. Accordingly, the $VM_{correct}>VM_{incorrect}$ contrast revealed subthreshold ($p < .05$, uncorrected) activation in the right secondary visual cortex (Table 3, Figure 6).

3.3. ROI Results

According to our hypotheses, we extracted beta values from our first-level contrasts in functional ROIs of A1, SMA, pSTG, V1, MT, SPL, and PMd. Per contrast and ROI, we first calculated one-sample *t*-tests to assess general activation or deactivation within ROIs before and after the training period (Figure S1).

For the AM>NOM contrast, one-sample *t*-tests revealed a significant deactivation in A1 before ($t(64) = -6.00$, $p < .001$, $d = -0.744$) and after training ($t(64) = -6.35$, $p < .001$, $d = -0.788$) and a significant activation before training in SMA ($t(64) = 3.02$, $p = .036$, $d = 0.375$), after training in V1 ($t(64) = 3.41$, $p = .006$, $d = 0.423$), and in MT before ($t(64) = 23.71$, $p < .001$, $d = 2.94$) and after ($t(64) = 22.49$, $p < .001$, $d = 2.79$) training.

For the VM>NOM contrast, one-sample *t*-tests showed significant activation before and after training in A1 (Pre: $t(64) = 8.74$, $p < .001$, $d = 1.084$; Post: $t(64) = 12.12$, $p < .001$, $d = 1.504$), pSTG (Pre: $t(64) = 13.77$, $p < .001$, $d = 1.708$; Post: $t(64) = 15.14$, $p < .001$, $d = 1.878$), V1 (Pre: $t(64) = 8.505$, $p < .001$, $d = 1.055$; Post: $t(64) = 8.304$, $p < .001$, $d = 1.030$), SMA (Pre: $t(64) = 5.83$, $p < .001$, $d = 0.722$; Post: $t(64) = 2.82$, $p = .032$, $d = 0.349$), MT (Pre: $t(64) = 7.08$, $p < .001$, $d = 0.878$; Post: $t(64) = 6.99$, $p < .001$, $d = 0.867$) and before training in PMd ($t(64) = 4.25$, $p < .001$, $d = 0.427$).

For the AM>AVM contrast, we found significant activation before ($t(64) = 21.64$, $p < .001$, $d = 2.683$) and after training ($t(64) = 21.71$, $p < .001$, $d = 2.692$) in MT, and significant deactivation in STG ($t(64) = -3.671$, $p = .005$, $d = -0.455$) and SMA ($t(64) = -3.277$, $p = .017$, $d = -0.406$) before training.

In the VM>AVM contrast, significant activation before and after training was found in A1 (Pre: $t(64) = 18.83$, $p < .001$, $d = 2.336$; Post: $t(64) = 19.07$, $p < .001$, $d = 2.366$) and pSTG (Pre: $t(64) = 16.47$, $p < .001$, $d = 2.043$; Post: $t(64) = 14.46$, $p < .001$, $d = 1.793$).

Lastly, for the NOM>SCB contrast, one-sample *t*-tests revealed significant deactivation in pSTG before ($t(64) = -4.03$, $p = .001$, $d = -0.500$) and after training ($t(64) = -5.72$, $p < .001$, $d = -0.710$) and in A1 after

Table 1
Peak coordinates for the contrasts VM>NOM, VM>AVM, AM>NOM, AM>AVM, and NOM>SCB from GLM1.

Localization	H	Cluster extent	MNI coordinates			*t* value
			x	y	z	
VM>NOM (FDR *p* <.0001)						
Supplementary motor area	R	389	5.5	8	57.5	6.48
Superior frontal sulcus	R	l.m.	13	5.5	70	5.98
Supplementary motor area	L	l.m.	-4.5	5.5	62.5	5.46
Medial frontal gyrus	L	l.m.	-9.5	10.5	45	4.44
Cingulate sulcus	R	l.m.	10.5	13	37.5	4.41
BA 4	L	65	-4.5	-27	57.5	4.80
	R	l.m.	5.5	-22	55	4.57
Supramarginal gyrus / BA 40	L	45	-52	-42	52.5	5.01
Precuneus	R	58	8	-44.5	50	6.05
Intraparietal sulcus	R	76	25.5	-59.5	42.5	5.28
Superior temporal gyrus (bilaterally extending into V1 and area MT)	R	17000	60.5	-39.5	17.5	15.57
Lingual gyrus / BA 18	L	l.m.	-9.5	-79.5	-7.5	14.67
Superior temporal gyrus (A2) extending into Heschl's gyrus (A1)	L	l.m.	-57	-34.5	15	14.53
Lingual gyrus / BA 18	R	l.m.	10.5	-77	-5	13.79
Superior temporal gyrus (A2) extending into Heschl's gyrus (A1)	R	l.m.	58	-17	7.5	13.72
Anterior Insula	L	72	-32	23	7.5	6.28
	R	38	35.5	25.5	5	4.69
VM>AVM (FDR *p* <.0001)						
Precentral gyrus / BA 4	R	23	53	-2	47.5	6.15
Heschl's gyrus (A1)	L	1435	-47	-22	7.5	17.73
	R	1684	53	-17	7.5	17.34
Superior temporal gyrus	R	l.m.	43	3	-17.5	5.38
AM>NOM (FDR *p* <.0001)						
Postcentral gyrus / S1	R	28	23	-34.5	62.5	4.77
S1 / BA 3	R	l.m.	15.5	-39.5	67.5	4.53
Putamen	L	277	-27	-7	7.5	5.96
Amygdala	L	l.m.	-27	-4.5	-17.5	5.47
Caudate nucleus (head)	L	l.m.	-12	13	0	4.62
Middle temporal gyrus (area MT / V5: also extending into dorsal premotor cortex and superior parietal lobule)	R	6693	48	-69.5	2.5	25.27
V1	R	l.m.	28	-92	5	23.34
Inferior temporal gyrus	R	l.m.	43	-57	-12.5	17.31
Inferior occipital gyrus / BA 19	R	l.m.	35.5	-82	-12.5	15.61
Thalamus	R	28	20.5	-29.5	2.5	5.73
V1 (also extending into dorsal premotor cortex and superior parietal lobule)	L	6018	-27	-92	-2.5	23.78
Middle occipital gyrus	L	l.m.	-42	-82	2.5	17.76
Fusiform gyrus	L	l.m.	-39.5	-52	-15	12.32
Cerebellum	L	l.m.	-12	-74.5	-42.5	7.94
Precentral gyrus / M1	L	l.m.	-49.5	-2	40	7.86
Amygdala	R	434	30.5	-4.5	-17.5	7.80
Putamen	R	l.m.	30.5	-12	0	7.14
AM>AVM (FDR *p* <.0001)						
Intraparietal sulcus, ascending segment	R	107	33	-39.5	57.5	5.87
BA 7	R	l.m.	28	-49.5	60	5.74
Intraparietal sulcus, ascending segment	L	102	-32	-39.5	55	5.95
Supramarginal gyrus / BA 40	R	107	53	-32	25	6.66
Supramarginal gyrus	L	64	-47	-32	22.5	7.34
Posterior cinuglate gyrus	L	54	-4.5	-52	22.5	5.16
Thalamus	R	64	20.5	-29.5	0	8.26
	L	64	-19.5	-29.5	-2.5	8.68
V1	R	1925	28	-94.5	-5	26.75
Middle temporal gyrus (area MT / V5)	R	l.m.	45.5	-72	0	21.08
Inferior temporal gyrus	R	l.m.	43	-49.5	-15	11.48
V1	L	1669	-24.5	-94.5	-7.5	28.67
Middle temporal gyrus (area MT / V5)	L	l.m.	-42	-69.5	5	16.63
Inferior temporal gyrus	L	l.m.	-42	-47	-17.5	9.14
Inferior frontal gyrus (pars orbitalis)	R	56	43	33	-15	6.86
	L	77	-44.5	28	-15	6.16
Cerebellum	R	24	0.5	-54.5	-37.5	6.21
NOM>SCB (FDR *p* <.0001)						
Superior frontal gyrus	R	375	18	43	45	6.60
Superior frontal sulcus	R	l.m.	25.5	25.5	47.5	5.74
Middle frontal gyrus	R	l.m.	35.5	20.5	42.5	5.72
Superior frontal sulcus	L	157	-22	23	45	6.03
	L	l.m.	-9.5	33	60	5.56
Angular gyrus	R	252	53	-64.5	32.5	7.45
BA 19	R	l.m.	43	-74.5	40	5.52
Angular gyrus / BA 39	L	318	-49.5	-69.5	32.5	6.23
Supramarginal gyrus	L	l.m.	-44.5	-54.5	27.5	6.18
Posterior superior temporal sulcus	L	l.m.	-52	-57	25	6.07
BA 19	L	l.m.	-42	-74.5	37.5	5.99
Posterior cingulate cortex	R	174	8	-52	30	5.56
Posterior cingulate cortex / BA 31	L	l.m.	-4.5	-49.5	30	5.32
Cingulate gyrus / BA 30	R	l.m.	3	-49.5	20	5.12
Superior frontal gyrus, medial part	L	841	-2	63	17.5	6.62
Superior frontal gyrus	R	l.m.	20.5	63	17.5	6.13
BA 9	L	l.m.	-4.5	53	42.5	5.95
V1	L	53	-22	-99.5	5	6.28
Inferior frontal gyrus (pars orbitalis)	R	87	43	35.5	-15	6.18

Note. H = Hemisphere, MNI = Montreal Neurological Institute, L = Left, R = Right, BA = Brodmann Area, l.m. = local maximum, V1 = primary visual cortex, M1 = primary motor cortex. Only clusters with a minimum extent of 20 voxels are reported.

training ($t(64) = -3.35$, $p = .014$, $d = -0.415$). Significant activation was present in V1 before training ($t(64) = 3.18$, $p = .023$, $d = 0.395$).

Additionally, we conducted rmANOVAs with the factor Time and the covariates Gender and MIA per ROI and contrast (Figure S1).

For the AM>NOM contrast, the rmANOVA revealed no significant effects in A1, V1, and pSTG. A significant effect of Gender was found in SMA ($F(1, 62) = 6.42$, $p = .014$, $\eta_p^2 = .094$), MT ($F(1, 62) = 10.13$, $p = .002$, $\eta_p^2 = .140$), SPL ($F(1, 62) = 4.91$, $p = .030$, $\eta_p^2 = .073$), and PMd ($F(1, 62) = 8.22$, $p = .006$, $\eta_p^2 = .117$), driven by higher beta values for women than for men in these ROIs. Furthermore, there was a significant effect of Time in MT ($F(1, 62) = 4.01$, $p = 0.05$, $\eta_p^2 = .061$), due to higher beta values before training.

The rmANOVA for the VM>NOM contrast did not reveal significant effects in A1. In pSTG, there was a significant effect of MIA ($F(1, 62) = 5.59$, $p = .021$, $\eta_p^2 = 0.083$), and in MT ($F(1, 62) = 5.47$, $p = .023$, $\eta_p^2 = 0.081$), PMd ($F(1, 62) = 4.33$, $p = .042$, $\eta_p^2 = 0.065$), and SPL ($F(1, 62) = 4.51$, $p = .038$, $\eta_p^2 = 0.068$), we found significant interactions of Time x MIA. Significant effects of Time were detected in SMA ($F(1, 62) = 9.92$, $p = .003$, $\eta_p^2 = 0.138$) and PMd ($F(1, 62) = 11.72$, $p = .001$, $\eta_p^2 = 0.159$), driven by higher beta values before training. Furthermore, there was a significant effect of Gender in V1 ($F(1, 62) = 12.25$, $p < .001$, $\eta_p^2 = .165$), as women had higher beta values than men.

For the AM>AVM contrast, the rmANOVA showed a significant effect of time in V1 ($F(1, 62) = 6.46$, $p = .027$, $\eta_p^2 = .094$) due to lower beta values before than after training. Additionally, there was a significant effect of Gender in MT ($F(1, 62) = 10.15$, $p = .002$, $\eta_p^2 = 0.141$), driven by higher beta values for women than men.

In the VM>AVM contrast, the only significant effect was found for MIA in V1 ($F(1, 62) = 5.48$, $p = .022$, $\eta_p^2 = .081$).

Lastly, for the NOM>SCB contrast, there was a significant effect of Time in SMA ($F(1, 62) = 5.97$, $p = .017$, $\eta_p^2 = 0.088$) due to lower beta

Table 2
Peak coordinates for the Pre>Post training comparisons for the NOM>SCB and VM>NOM contrasts from GLM1.

Localization	H	Cluster extent	MNI coordinates			*t* value
			x	y	z	
Pre>Post for NOM>SCB (FDR *p* <.05)						
Superior parietal lobule / BA 5	R	24	20.5	-49.5	67.5	3.37
Superior frontal gyrus	R	41	20.5	43	47.5	3.36
Superior frontal sulcus	R	l.m.	23	38	40	3.29
Middle cingulate cortex	R	37	5.5	-19.5	40	3.79
	L	l.m.	-7	-14.5	40	2.99
Angular gyrus / BA 39	R	94	48	-72	32.5	4.24
Middle occipital gyrus	L	150	-39.5	-69.5	27.5	3.52
Angular gyrus	L	l.m.	-52	-62	32.5	2.95
BA 19	L	l.m.	-39.5	-74.5	37.5	2.93
Parieto-occipital sulcus	L	2995	-7	-64.5	15	5.38
Precuneus	R	l.m.	10.5	-57	27.5	5.34
Cuneus	R	l.m.	10.5	-84.5	32.5	5.31
Parieto-occipital sulcus	R	l.m.	0.5	-74.5	30	4.83
Cuneus	L	l.m.	-12	-87	32.5	4.77
Medial prefrontal cortex	R	838	5.5	58	-2.5	4.55
Superior frontal sulcus, medial part	L	l.m.	-2	63	17.5	4.26
Medial prefrontal cortex	L	l.m.	-9.5	55.5	10	4.06
BA 25	L	l.m.	-4.5	23	-17.5	3.89
Anterior cingulate cortex	R	l.m.	3	40.5	2.5	3.49
Inferior temporal sulcus	L	20	-59.5	-19.5	-12.5	3.16
Cerebellum	R	24	20.5	-87	-25	3.48
Middle temporal gyrus / BA 21	L	38	-54.5	8	-27.5	3.71
Middle temporal gyrus	R	211	48	13	-37.5	5.11
Pre>Post for VM>NOM (FDR *p* <.05)						
Superior frontal sulcus	L	38	-22	5.5	57.5	3.96
Supplementary motor area	R	584	3	15.5	52.5	5.32
Middle frontal gyrus	R	l.m.	38	5.5	55	4.39
Superior frontal sulcus / PMd	R	l.m.	23	3	57.5	3.71
Inferior frontal junction	L	21	-52	10.5	17.5	3.63
Middle frontal gyrus	R	108	35.5	50.5	15	4.61
	L	73	-42	45.5	15	4.06
Anterior insula	L	74	-32	28	0	5.21
	R	94	33	25.5	0	4.02

Note. H = Hemisphere, MNI = Montreal Neurological Institute, L = Left, R = Right, BA = Brodmann Area, l.m. = local maximum, PMd = dorsal premotor cortex. Only clusters with a minimum extent of 20 voxels are reported.

values before training.

To better understand the influence of individual hurdling performance improvement on brain activation, we used exploratory Pearson correlations to further analyze any (interaction) effects found for MIA. A main effect of MIA was detected for the VM>NOM contrast in pSTG and for the VM>AVM contrast in V1. In both ROIs, there was a non-significant trend for a negative correlation of MIA and beta values ($pSTG_{VM>NOM}$: $r = -.327$, $p = .063$; $V1_{VM>AVM}$: $r = -.329$, $p = .059$), i.e., participants with lower performance increases in hurdling had higher brain activation. An interaction effect of Time and MIA was observed for the VM>NOM contrast in MT, SPL, and PMd. Descriptively, we observed a negative association between MIA and beta values only before, but not after, hurdling training in these ROIs. However, the negative correlation only reached significance in MT (Pre: $r = -.351$, $p = .033$; Post: $r = -.084$, $p = 1$), but not the other ROIs (SPL_{Pre}: $r = -.185$, $p = 1$; SPL_{Post}: $r = .007$, $p = 1$; PMd_{Pre}: $r = -.229$, $p = .532$; PMd_{Post}: $r = -.002$, $p = 1$).

4. Discussion

The present study investigated visual and auditory prediction in hurdling using fMRI within a pre-post training design. Participants watched point-light hurdling videos while visual and/or auditory information was briefly masked, requiring them to rely on internal models, or the remaining modality, during a movement prediction task. Between sessions, participants completed six weeks of hurdling training to strengthen their own sensorimotor hurdling models. We found that prediction accuracy declined when sensory input was masked. At the same time, the brain flexibly recruited modality-specific networks depending on the available input. As expected, under visual masking, the brain not only relied more on the remaining auditory stream but also engaged frontal, motor, and visual regions despite the absence of visual input, hinting at top-down visual prediction. In contrast, auditory masking increased recruitment in visual regions but showed no significant evidence for an auditory analogue of the top-down effect seen under visual masking. Consistent with this asymmetry, behavioral costs were largest under auditory masking. On correctly solved no-sound trials, we observed increases in the early auditory cortex, though this transient recruitment showed no robust group-level effect. Following hurdling training, predictive accuracy improved, and training-related changes in neural activation overlapped with the systems recruited under visual masking in frontal control and visuomotor nodes, consistent with more efficient internal models for visual prediction. Taken together, the findings support a visually anchored predictive architecture that is sharpened by practice. The following sections detail the behavioral asymmetry, neural markers of top-down visual prediction, candidate reasons for the absent auditory counterpart, and training-related efficiency gains.

4.1. *Predicting unfolding movement: The role of audiovisual input and motor expertise*

Behaviorally, our results reveal that both visual and auditory information are integral to accurate movement prediction. Accuracy declined under all masking conditions compared to the no-mask control, with participants performing least accurately in the auditory mask condition among the masked conditions. Moreover, participants were particularly slow in responding when auditory information was absent. These findings align with previous work showing auditory input is a critical source of temporal information, for example, in beat sensitivity tasks (Grahn, 2012). Importantly, we observed the expected overall increase in accuracy and faster reaction times after hurdle training, indicating that motor expertise strengthens reliance on internal predictive models in a movement speed prediction task. Notably, gains were especially evident in masked conditions, while no significant improvements emerged in the no-mask or scrambled control trials. This pattern is consistent with prior evidence showing expertise allows athletes to extract highly specific movement cues, even within occlusion paradigms (Abernethy et al., 2001; Williams et al., 2011). Thus, training appears to enhance the capacity to cope with missing information by consolidating an internal predictive model of hurdling, whereas scrambled sequences, as expected, did not benefit from expertise, as they lack a meaningful movement structure to predict.

4.2. *Using what is left: Flexible selection of available sensory information*

We observed the expected decrease in A1 activity when auditory input was masked compared with the no-mask condition. Conversely, when *only* auditory information was available (i.e., visual masking), activity increased in A1, SMA, and STG relative to no-mask, consistent with leveraging auditory evidence and sensorimotor prediction (Chennu et al., 2016; Heins et al., 2020a,b; Jo et al., 2019). On the visual side, visual masking produced the expected decrease in V1 relative to no mask. When *only* visual information was available (i.e., auditory masking), we observed increased activation across visual cortices, including area MT, SPL, and PMd, relative to no mask. Taken together, these patterns indicate increased recruitment of the auditory network when visual information is missing and of the visual network when auditory information is missing, alongside reduced activity in the primary cortex of the occluded modality. These findings provide evidence

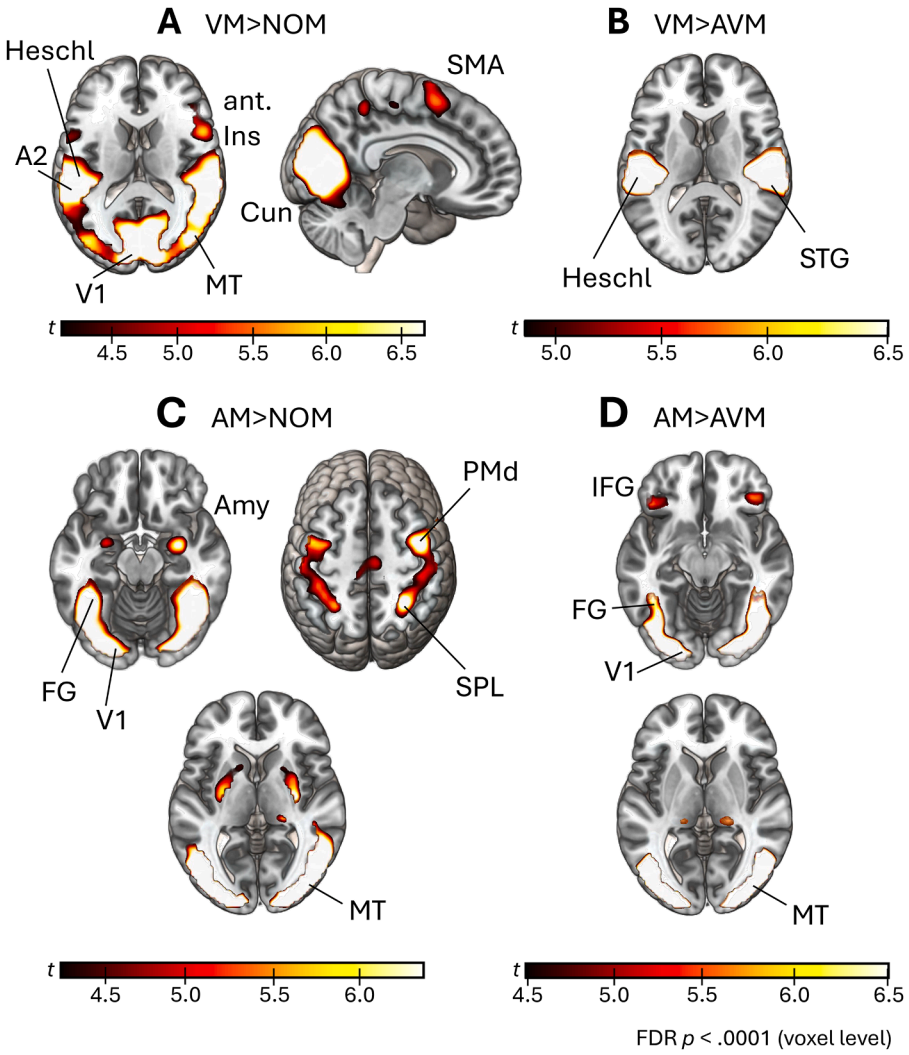

Figure 4. Whole brain results for the contrasts VM>NOM, VM>AVM, AM>NOM, and AM>AVM from GLM1.
Note. All contrasts are presented at FDR (p<.0001) (voxel level). A2 = secondary auditory cortex, STG = superior temporal gyrus, V1 = primary visual cortex, Area MT = middle temporal area/V5, SMA = supplementary motor area, FG = fusiform gyrus, Amy = Amygdala, IFG = inferior frontal gyrus, Cun = Cuneus, ant. Ins = anterior Insula, SPL = superior parietal lobule, PMd = dorsal premotor area.

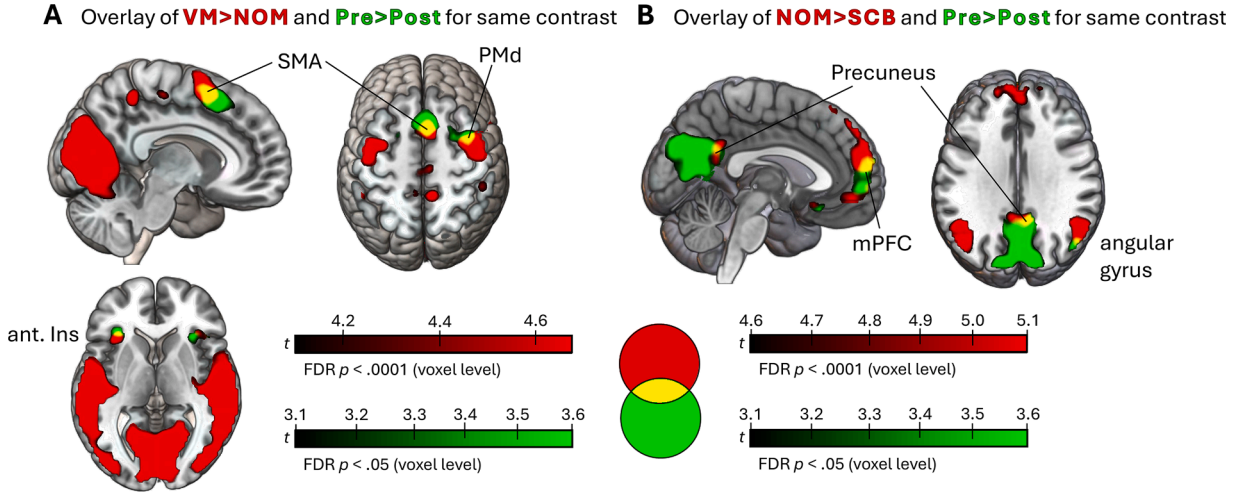

Figure 5. Overlay for the contrasts VM>NOM (A) and NOM>SCB (B) from GLM1 with their respective Pre>Post training activation contrasts.
Note. SMA = supplementary motor area, PMd = dorsal premotor area, mPFC = medial prefrontal cortex, ant. Ins = anterior Insula.

Table 3
Peak coordinates for the contrasts $VM_{correct}>VM_{incorrect}$ and $AM_{correct}>AM_{incorrect}$ from GLM2.

Localization	H	Cluster extent	MNI coordinates			*t* value
			x	y	z	
$VM_{correct}>VM_{incorrect}$ (uncorrected at $p < .05$)						
V2, extending into V1	R	217	25.5	-97	10	2.51
$AM_{correct}>AM_{incorrect}$ (uncorrected at $p < .05$)						
Supramarginal gyrus	L	81	-52	-37	47.5	2.68
Posterior insula	R	73	35.5	-9.5	20	2.26
Middle frontal gyrus	L	31	-42	45.5	17.5	2.47
Superior temporal gyrus (A2)	R	362	53	-24.5	10	2.91
Heschl's gyrus (A1)	R	l.m.	35.5	-27	10	1.83
Superior temporal gyrus (A2), extending into Heschl's gyrus (A1)	L	353	-49.5	-24.5	2.5	3.03
Inferior frontal gyrus (pars triangularis)	R	101	50.5	38	5	3.24
Putamen	R	69	23	3	-5	2.17
Parahippocampal gyrus	R	28	20.5	-2	-22.5	2.06
Amygdala	R	l.m.	30.5	-2	-20	1.99
Cerebellum	R	32	20.5	-54.5	-45	2.17

Note. H = Hemisphere, MNI = Montreal Neurological Institute, L = Left, R = Right, l.m. = local maximum. A1 = primary auditory cortex, A2 = secondary auditory cortex, V1 = primary visual cortex, V2 = secondary visual cortex.

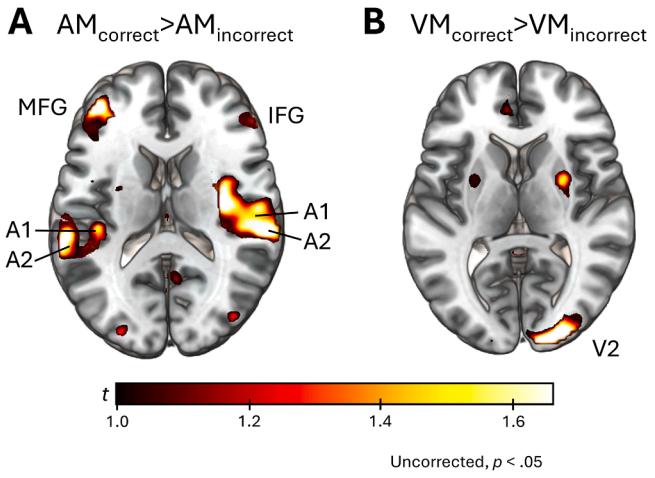

Figure 6. Whole brain results for the contrasts $AM_{correct}>AM_{incorrect}$ and $VM_{correct}>VM_{incorrect}$ from GLM2.
Note. MFG = middle frontal gyrus, IFG = inferior frontal gyrus, A1= primary auditory cortex, A2 = secondary auditory cortex, V2 = secondary visual cortex. Subthreshold (uncorrected, $p < .05$) findings are depicted here.

that the brain relies on the available modality and flexibly selects sensory input to inform internal models during transient deprivation (Andersson et al., 2019; Chennu et al., 2016; Heins et al., 2020a,b; Jo et al., 2019; Maes et al., 2020). This increase in bottom-up sensory processing might be modulated by top-down re-orientation of attention to the available modality, or related to an upregulation of the prediction error gain for the remaining modality, which we cannot differentiate with the current study.

4.3. Supplementing missing information: The asymmetry of visual and auditory prediction

Interestingly and beyond this shifting, visual masking also yielded additional engagement of visual areas despite the absence of visual input, which cannot be explained by residual sensory drive, or attentional mechanisms, for which also activation in higher-order attention networks would be expected (e.g., Posner & Rothbart, 2007; Posner, 2012). Previous studies have shown that in the absence of visual input, participants can generate mental images that evoke activity in corresponding visual areas (Ishai et al., 2000; Kosslyn & Thompson, 2003; Stokes et al., 2009). We did not directly assess whether participants used sensory imagery, and they were not instructed to do so. Importantly, neural activation patterns alone do not prove imagery or prediction (Hubbard, 2010; Zatorre & Halpern, 2005). That said, explicit, conscious imagery is not required - predictive processes can occur automatically and outside awareness (Ford & Mathalon, 2012; Tivadar et al., 2021). Additionally, Chennu et al. (2016) argue that paradigms with omitted sensory input provide a direct measure of top-down sensory prediction. Accordingly, we interpret the extra visual activity during visual masking as the internal predictive model generating the missing visual input via top-down prediction, in line with reports of imagery-related activations in similar regions (e.g., Andersson et al., 2019; Ganis et al., 2004; Guillot et al., 2009). Supporting this interpretation, better individual performance during visually masked trials was associated (albeit subthreshold at the group level) with greater activation in the visual cortex. Interestingly, when only visual information was available, we also found increased activation in the cerebellum, an important hub for motor prediction (e.g., Nixon & Passingham, 2001; Ebner & Pasalar, 2008). The cerebellum is known to be involved in the prediction of sensory consequences of motor commands, as well as the computation of prediction errors when these predictions do not match sensory feedback (Popa & Ebner, 2019). Thus, activation detected here can be taken as a further hint for ongoing predictive processes concerning the visual modality in hurdling perception. However, we would like to highlight once again that this study was not designed in an optimal way to investigate cerebellar mechanisms. To this end, these findings, and, more importantly, the lack of more prominent cerebellar activations throughout the study, should be interpreted with caution.

In contrast, we did not observe a comparable up-regulation within the auditory association cortex or SMA during auditory masking that might have been expected as part of top-down predictive substitution of missing auditory input (Lima et al., 2016). Unlike earlier imagery studies, participants were not instructed to imagine the missing sounds, allowing us to assess spontaneous neural responses. In contrast to earlier studies that reported SMA and pSTG activity during the prediction of self-generated sounds (Guenther & Hickok, 2015; Jo et al., 2019; Oestreich et al., 2018; Waszak et al., 2012), our paradigm did not involve speech, music, or auditory feedback to button presses. Instead, we used hurdling as a whole-body movement in which sounds occurred incidentally rather than intentionally. This distinction is important, since the brain is generally quite effective at interpolating beats and maintaining performance under auditory masking when sounds are intentionally produced, such as in speech or music (Finney, 1997; Repp, 1999; Tal et al., 2017). In hurdling, by contrast, the sounds are rhythmically structured but incidental to the action, and this lack of intentional sound production may limit their use as a basis for predictive compensation. Consistent with this interpretation, previous work showed that auditory scrambling impaired evaluation of intentional (tap dancing) more than incidental (hurdling) sounds, with stronger SMA and pSTG activation for tap dancing, and that temporal delays in these sounds elicited transient increases in pSTG activity and stronger pSTG–SMA coupling, with SMA showing an additional delay-related increase for tap dancing (Heins et al., 2020a,b). Together, these findings suggest that incidental sounds may not provide a sufficiently reliable basis for auditory prediction, offering a plausible explanation for the present null result.

Notably, we did observe subthreshold activation in A1, STG, left medial frontal gyrus, and right inferior frontal gyrus on correctly answered auditory-masked trials compared to incorrect responses during auditory masking. Paralleling the findings for visually masked trials, this might indicate that to some degree, the brain is able to supplement missing auditory information by using top-down predictive processes

and that the degree to which it does is behaviorally relevant. In line with this, auditory information is considered to be usually more critical for tasks involving rhythmic beat (Grahn, 2012), and our behavioral findings further supported this view by showing that performance suffered most when auditory input was masked. This suggests that auditory information was to some degree used for successful movement prediction, and while compensatory recruitment of other areas was detectable, this effect was not robust at the group level. Importantly, these findings need to be interpreted with caution due to their subthreshold nature and require further investigation. For example, individual variability in musical expertise or attentional strategies may play a role, a possibility that should be addressed in future studies.

4.4. On becoming a hurdler: Effects on auditory and visual prediction

If sensory masking compels reliance on top-down prediction, then regions recruited under masking should also be modulated by training once participants can draw on their own experience-shaped internal models. For visual masking, we observed precisely this pattern: The comparison between visual masking and no masking engaged visual cortices, motion-sensitive areas, and SMA. Training then reduced activation in SMA (ROI-confirmed) and a number of further frontal areas. Importantly, only SMA met both criteria, namely being recruited under visual masking and showing training-related modulation, identifying it as the strongest candidate region for experience-shaped predictive control in our task. SMA is a functionally heterogeneous region that contributes in a domain-general way to sequence processing (Shima & Tanji, 2000) across diverse domains, including action, timing, space, music, and language, by integrating sequential elements into higher-order representations, with pre-SMA and SMA-proper making distinct contributions (Cona & Semenza, 2017). At the same time, premotor areas, including SMA, have been described as serving both motor control and the prediction of forthcoming sensory consequences (afferent or reafferent; Schubotz, 2007). In this sense, SMA emerges as a key site where training-induced changes in predictive processing can be observed, bridging its general role in sequence integration with its specific role in anticipating sensory consequences of movement. However, evidence on SMA modulation during motor learning is somewhat mixed: while reviews emphasize that SMA activity often increases and pre-SMA decreases with practice (Dayan & Cohen, 2011), studies on motor expertise have instead reported reduced SMA recruitment during imagery of well-learned movements, interpreted as neural efficiency (Zhang et al., 2019). Our finding of reduced SMA activity after hurdling training aligns with this latter pattern, extending it to movement prediction under sensory masking. By contrast, we did not see comparable top-down signatures for auditory masking, nor parallel pre-post modulation tied to the auditory condition.

In sum, hurdling prediction appears to rely on a visually anchored, SMA-centered top-down mechanism sharpened by training, whereas no analogous auditory reinstatement was observed. This modality-specific asymmetry refines accounts of predictive control in complex action and highlights an important next step: delineating the task and context conditions under which auditory prediction is engaged.

4.5. Limitations and future directions

One limitation of our study is that all participants went through the hurdling training and we did not include a control group without a hurdling intervention. Thus, it cannot be completely ruled out that the behavioral and neural changes from the first to the second fMRI session were driven by simply becoming more familiar with the task rather than a strengthening of an embodied predictive model. However, this explanation seems insufficient to explain our findings. A control analysis on task improvement within the first fMRI session did not reveal significant improvement in accuracy or reaction times. This finding, together with the long time interval of six weeks between experimental sessions, makes it highly unlikely that participants' performance would increase due to a familiarization with the task alone. However, it will be highly interesting to compare our results to a group of participants who did not experience hurdling training in a future study.

In the present study, we demonstrated visual predictive processes in the absence of visual input, while finding only limited evidence for auditory prediction. This may reflect a genuine modality asymmetry, but task design could also have favored vision: hurdling can be performed using vision alone, whereas audition is not sufficient. Tasks emphasizing beat continuation or rhythmic movement contexts may be better suited to elicit auditory prediction (Kennel et al., 2015; Repp, 1999; Tal et al., 2017).

Another important limitation of our present study is the fact that due to a methodological constraint, namely the field of view during fMRI acquisition, we could not specifically test hypotheses about cerebellar involvement in the described processes, despite the relevance of this region in motor prediction (e.g., Nixon & Passingham, 2001; Ebner & Pasalar, 2008). While we did detect some cerebellar activation clusters, it is important to note that the lack of more prominent involvement of the cerebellum must not be interpreted as a non-involvement in the perceptual and predictive mechanisms described here, but can likely be attributed to signal loss in large parts of this brain region. We thus highly recommend repeating the study with an adjusted field of view to investigate cerebellar involvement in hurdling perception and prediction in more depth.

A further methodological consideration is the MRI environment: rhythmic scanner noise can reduce auditory BOLD responses (Gaab et al., 2007) and impair auditory task performance (Mazard et al., 2002). While unlikely to explain the full asymmetry, it may have contributed and should be controlled in future studies. For example, using sparse-sampling fMRI, which introduces silent delays between acquisition volumes, could help to overcome this problem (Perrachione and Ghosh, 2013).

Despite the considerable merit of our present results, the analyses were, for now, limited to univariate contrasts. Consequently, they do not allow us to determine how different regions interact with one another during modality-specific prediction. To better understand these networks, our next step is to examine directed connectivity (Dührkop et al., in preparation) using dynamic causal modeling (Friston et al., 2003).

As expected, we observed training-related changes in both brain activity and prediction accuracy that likely reflect the strengthening of an internal sensorimotor model of hurdling. A natural next step will be to ask whether such functional changes are accompanied by structural adaptations (Chang, 2014; Dayan & Cohen, 2011), for example, in terms of white matter connectivity or other characteristics of brain architecture, like the degree of myelination (Wang et al., 2023).

Finally, we observed that activity in regions commonly associated with social-cognitive functions, i.e., the TOM network (Brown & Brüne, 2012; Schurz et al., 2014), declined after training, as reflected in the baseline contrast no-mask vs. scrambled-movement. One intriguing possibility is that, as one's own sensorimotor model of hurdling consolidates, reliance on "other-minds" interpretive processes diminishes. Although this was not a primary focus of our study, it represents an exciting avenue for future research. On a related note, it is worth considering that visual stimuli were presented from a third-person perspective, while auditory stimuli were available from a quasi-first-person perspective. This could have influenced the degree to which participants identified with the point-light display depending on the sensory modality and, in turn, how they relied on visual and auditory information for their internal predictive model. Thus, it would be interesting to also use first-person videos of hurdling in future studies. Additionally, the abstract nature of the point-light videos might have influenced the participants' perception of the movement. Thus, future work should address how naturalistic hurdling displays affect the results reported here.

4.6. Conclusions

This study examined how the brain compensates for missing sensory information during observation of hurdling, a complex whole-body movement. Prediction accuracy dropped under both auditory and visual masking, but only visual masking elicited clear top-down recruitment of predictive networks. In contrast, auditory prediction showed only weak, subthreshold evidence, highlighting a potential asymmetry between modalities in this task. Hurdling training improved prediction under sensory masking and reduced SMA activity during visual occlusion, suggesting more efficient reliance on internal models. Together, these findings point to a visually anchored predictive architecture that can be sharpened through motor practice, while the conditions for robust auditory prediction remain to be clarified.

Funding Information

This work was supported by the German Research Foundation (Deutsche Forschungsgemeinschaft) under grant number 515997569. The funder had no role in study design, data collection, analysis and interpretation, decision to publish, or writing of the report.

Data availability

The data reported in this manuscript is publicly available in an OSF repository (https://osf.io/f7ahq/?view_only=d0bab406285347b89674357e0cb73053).

CRediT authorship contribution statement

Sophie Siestrup: Writing – review & editing, Writing – original draft, Visualization, Software, Project administration, Methodology, Investigation, Formal analysis, Data curation, Conceptualization. **Marc Dührkop:** Writing – review & editing, Writing – original draft, Visualization, Investigation, Formal analysis, Data curation. **Viviana Villafañe Barraza:** Writing – review & editing, Methodology, Investigation, Data curation. **Dennis Redlich:** Writing – review & editing, Project administration, Methodology, Investigation, Formal analysis, Data curation, Conceptualization. **Alexandra Pizzera:** Writing – review & editing, Methodology, Investigation, Funding acquisition, Data curation, Conceptualization. **Falko Mecklenbrauck:** Writing – review & editing, Software, Data curation. **Jochen Bauer:** Writing – review & editing, Software, Methodology. **Markus Raab:** Writing – review & editing, Supervision, Resources, Methodology, Funding acquisition, Conceptualization. **Ricarda I. Schubotz:** Writing – review & editing, Supervision, Resources, Methodology, Funding acquisition, Conceptualization.

Declaration of competing interest

The authors report there are no competing interests to declare.

Acknowledgments

We thank Monika Mertens, Lena Charlotte Innig, Thea Broering, Anna Sophia Asdonk, Pia Niedrée, Leon Exeler, Nina Liedtke, Marius Boeltzig, and Julian von Seydewitz for their help during MRI data collection, Juliane Diefenthal and Leon Exeler for help with the generation of stimulus material and Mustafa Acar for assistance with the hurdling paradigm. Further, we thank Lena Charlotte Innig for help with data processing and the track-and-field experts and lecturers at the German Sport University Cologne for advice concerning the hurdling training. We also want to thank Marc de Lussanet De La Sablonière for sharing expertise and resources concerning motion tracking. Lastly, we thank the Biological Psychology Group of the University of Münster as well as the Department of Performance Psychology of the German Sport University Cologne for helpful comments and valuable discussions.

Supplementary materials

Supplementary material associated with this article can be found, in the online version, at doi:10.1016/j.neuroimage.2025.121673.

References

Abernethy, B., Gill, D.P., Parks, S.L., Packer, S.T., 2001. Expertise and the perception of kinematic and situational probability information. Perception 30 (2), 233–252. https://doi.org/10.1068/p2872.

Andersson, J.L.R., Skare, S., Ashburner, J., 2003. How to correct susceptibility distortions in spin-echo echo-planar images: Application to diffusion tensor imaging. NeuroImage 20 (2), 870–888. https://doi.org/10.1016/S1053-8119(03)00336-7.

Andersson, P., Ragni, F., Lingnau, A., 2019. Visual imagery during real-time fMRI neurofeedback from occipital and superior parietal cortex. NeuroImage 200, 332–343. https://doi.org/10.1016/j.neuroimage.2019.06.057.

Brett, M., Anton, J.-L., Valabregue, R., Poline, J.-B, 2002. Region of interest analysis using an SPM tollboox (abstract). In: Presented at the 8th international Conference on Functional Mapping of the Human Brain. Sendai, Japan.

Brich, L.F.M., Bächle, C., Hermsdörfer, J., Stadler, W., 2018. Real-time prediction of observed action requires integrity of the dorsal premotor cortex: Evidence from repetitive transcranial magnetic stimulation. Frontiers in Human Neuroscience 12, 101. https://doi.org/10.3389/fnhum.2018.00101.

Brown, E.C., Brüne, M., 2012. The role of prediction in social neuroscience. Frontiers in Human Neuroscience 6, 147. https://doi.org/10.3389/fnhum.2012.00147.

Chang, Y., 2014. Reorganization and plastic changes of the human brain associated with skill learning and expertise. Frontiers in Human Neuroscience 8, 35. https://doi.org/10.3389/fnhum.2014.00035.

Chennu, S., Noreika, V., Gueorguiev, D., Shtyrov, Y., Bekinschtein, T.A., Henson, R., 2016. Silent expectations: Dynamic causal modeling of cortical prediction and attention to sounds that weren't. The Journal of Neuroscience 36 (32), 8305–8316. https://doi.org/10.1523/JNEUROSCI.1125-16.2016.

Clark, A., 2013. Whatever next? Predictive brains, situated agents, and the future of cognitive science. Behavioral and Brain Sciences 36, 181–204. https://doi.org/10.1017/S0140525X12000477.

Cona, G., Semenza, C., 2017. Supplementary motor area as key structure for domain-general sequence processing: A unified account. Neuroscience and Biobehavioral Reviews 72, 28–42. https://doi.org/10.1016/j.neubiorev.2016.10.033.

Dai, S., 2021. Handling missing responses in psychometrics: Methods and software. Psych 3 (4), 673–693. https://doi.org/10.3390/psych3040043.

Dayan, E., Cohen, L.G., 2011. Neuroplasticity subserving motor skill learning. Neuron 72 (3), 443–454. https://doi.org/10.1016/j.neuron.2011.10.008.

De Ayala, R.J., Plake, B.S., Impara, J.C., 2001. The impact of omitted responses on the accuracy of ability estimation in item response theory. Journal of Educational Measurement 38 (3), 213–234. https://doi.org/10.1111/j.1745-3984.2001.tb01124.x.

Diersch, N., Jones, A.L., Cross, E.S., 2016. The timing and precision of action prediction in the aging brain. Human Brain Mapping 37 (1), 54–66. https://doi.org/10.1002/hbm.23012.

Ebner, T.J., Pasalar, S., 2008. Cerebellum predicts the future motor state. Cerebellum 7 (4), 583–588. https://doi.org/10.1007/s12311-008-0059-3.

Erdfelder, E., Faul, F., Buchner, A., 1996. GPOWER: a general power analysis program. Behavior Research Methods, Instruments, & Computers 28, 1–11. https://doi.org/10.3758/BF03203630.

Finney Steven, A., 1997. Auditory feedback and musical keyboard performance. Music Perception 15 (2), 153–174. https://doi.org/10.2307/40285747.

Ford, J.M., Mathalon, D.H., 2012. Anticipating the future: Automatic prediction failures in schizophrenia. International Journal of Psychophysiology 83 (2), 232–239. https://doi.org/10.1016/j.ijpsycho.2011.09.004.

Friston, K.J., Harrison, L., Penny, W., 2003. Dynamic causal modelling. NeuroImage 19 (4), 1273–1302. https://doi.org/10.1016/S1053-8119(03)00202-7.

Friston, K.J., Holmes, A.P., Worsley, K.J., Poline, J.-P., Frith, C.D., Frackowiak, R.S.J, 1994. Statistical parametric maps in functional imaging: A general linear approach. Human Brain Mapping 2 (4), 189–210. https://doi.org/10.1002/hbm.460020402.

Friston, K., 2005. A theory of cortical responses. Philosophical Transactions of the Royal Society B 360 (1456), 815–836. https://doi.org/10.1098/rstb.2005.1622.

Friston, K., 2012. Prediction, perception and agency. International Journal of Psychophysiology 83 (2), 248–252. https://doi.org/10.1016/j.ijpsycho.2011.11.014.

Gaab, N., Gabrieli, J.D.E., Glover, G.H., 2007. Assessing the influence of scanner background noise on auditory processing. I. An fMRI study comparing three experimental designs with varying degrees of scanner noise. Human Brain Mapping 28 (8), 703–720. https://doi.org/10.1002/hbm.20298.

Ganis, G., Thompson, W.L., Kosslyn, S.M., 2004. Brain areas underlying visual mental imagery and visual perception: An fMRI study. Cognitive Brain Research 20 (2), 226–241. https://doi.org/10.1016/j.cogbrainres.2004.02.012.

Genovese, C.R., Lazar, N.A., Nichols, T., 2002. Thresholding of statistical maps in functional neuroimaging using the false discovery rate. NeuroImage 15 (4), 870–878. https://doi.org/10.1006/nimg.2001.1037.

Grahn, J.A., 2012. See what I hear? Beat perception in auditory and visual rhythms. Experimental Brain Research 220 (1), 51–61. https://doi.org/10.1007/s00221-012-3114-8.
Grosbras, M.-H., Beaton, S., Eickhoff, S.B., 2012. Brain regions involved in human movement perception: A quantitative voxel-based meta-analysis. Human Brain Mapping 33, 431–454.doi. https://doi.org/10.1002/hbm.21222.
Guenther, F.H., Hickok, G., 2015. Role of the auditory system in speech production. Handbook of Clinical Neurology 129, 161–175. https://doi.org/10.1016/B978-0-444-62630-1.00009-3.
Guilfoyle, D.N., Dyakin, V.V., O'Shea, J., Pell, G.S., Helpern, J.A., 2003. Quantitative measurements of proton spin-lattice (T1) and spin-spin (T2) relaxation times in the mouse brain at 7.0 T. Magnetic Resonance in Medicine 49 (3), 576–580. https://doi.org/10.1002/mrm.10371.
Guillot, A., Collet, C., Nguyen, V.A., Malouin, F., Richards, C., Doyon, J., 2009. Brain activity during visual versus kinesthetic imagery: An fMRI study. Human Brain Mapping 30 (7), 2157–2172. https://doi.org/10.1002/hbm.20658.
Heins, N., Pomp, J., Kluger, D.S., Trempler, I., Zentgraf, K., Raab, M., Schubotz, R.I., 2020a. Incidental or intentional? Different brain responses to one's own action sounds in hurdling vs. tap dancing. Frontiers in Neuroscience 14, 483. https://doi.org/10.3389/fnins.2020.00483.
Heins, N., Trempler, I., Zentgraf, K., Raab, M., Schubotz, R.I., 2020b. Too late! Influence of temporal delay on the neural processing of one's own incidental and intentional action-induced sounds. Frontiers in Neuroscience 14, 573970. https://doi.org/10.3389/fnins.2020.573970.
Hubbard, T.L., 2010. Auditory imagery: Empirical findings. Psychological Bulletin 136 (2), 302–329. https://doi.org/10.1037/a0018436.
Ishai, A., Ungerleider, L.G., Haxby, J.V., 2000. Distributed neural systems for the generation of visual images. Neuron 28 (3), 979–990. https://doi.org/10.1016/s0896-6273(00)00168-9.
Jenkinson, M., Beckmann, C.F., Behrens, T.E., Woolrich, M.W., Smith, S.M., 2012. FSL. NeuroImage 62 (2), 782–790. https://doi.org/10.1016/j.neuroimage.2011.09.015.
Jo, H.-G., Habel, U., Schmidt, S., 2019. Role of the supplementary motor area in auditory sensory attenuation. Brain Structure & Function 224 (7), 2577–2586. https://doi.org/10.1007/s00429-019-01920-x.
Kaisidou, V., Gaitanidis, L., Panoutsakopoulos, V., 2021. Relationship between the technique index and perfromance in 60-m hurdle indoor races in elite male heptathletes. TRENDS in Sport Sciences 28 (2). https://doi.org/10.23829/TSS.2021.28.2-7.
Kennel, C., Pizzera, A., Hohmann, T., Schubotz, R.I., Murgia, M., Agostini, T., Raab, M., 2014. The perception of natural and modulated movement sounds. Perception 43 (8), 796–804. https://doi.org/10.1068/p7643.
Kennel, C., Streese, L., Pizzera, A., Justen, C., Hohmann, T., Raab, M., 2015. Auditory reafferences: The influence of real-time feedback on movement control. Frontiers in Psychology 6, 69. https://doi.org/10.3389/fpsyg.2015.00069.
Kleiner, M., Brainard, D., Pelli, D., Ingling, A., Murray, R., Broussard, C., Cornelissen, F., 2007. What's new in psytoolbox-3? A free cross-platform toolkit for Psychophysics with Matlab & GNU/Octave.
Kosslyn, S.M., Thompson, W.L., 2003. When is early visual cortex activated during visual mental imagery? Psychological Bulletin 129 (5), 723–746. https://doi.org/10.1037/0033-2909.129.5.723.
Kowarik, A., Templ, M., 2016. Imputation with the R Package VIM. Journal of Statistical Software 74 (7). https://doi.org/10.18637/jss.v074.i07.
Kuhnke, P., Beaupain, M.C., Arola, J., Kiefer, M., Hartwigsen, G., 2023. Meta-analytic evidence for a novel hierarchical model of conceptual processing. Neuroscience and Biobehavioral Reviews 144, 104994. https://doi.org/10.1016/j.neubiorev.2022.104994.
Lima, C.F., Krishnan, S., Scott, S.K., 2016. Roles of supplementary motor areas in auditory processing and auditory imagery. Trends in Neurosciences 39 (8), 527–542. https://doi.org/10.1016/j.tins.2016.06.003.
MacPherson, A.C., Collins, D., Obhi, S.S., 2009. The importance of temporal structure and rhythm for the optimum performance of motor skills: A new focus for practitioners of sport psychology. Journal of Applied Sport Psychology 21 (S1), S48–S61. https://doi.org/10.1080/10413200802595930.
Maes, C., Swinnen, S.P., Albouy, G., Sunaert, S., Gooijers, J., Chalavi, S., Pauwels, L., 2020. The role of the PMd in task complexity: Functional connectivity is modulated by motor learning and age. Neurobiology of Aging 92, 12–27. https://doi.org/10.1016/j.neurobiolaging.2020.03.016.
Mazard, A., Mazoyer, B., Etard, O., Tzourio-Mazoyer, N., Kosslyn, S.M., Mellet, E., 2002. Impact of fMRI acoustic noise on the functional anatomy of visual mental imagery. Journal of Cognitive Neuroscience 14 (2), 172–186. https://doi.org/10.1162/089892902317236821.
Müller, F., Jauernig, L., Cañal-Bruland, R., 2019. The sound of speed: How grunting affects opponents' anticipation in tennis. PloS One 14 (4), e0214819. https://doi.org/10.1371/journal.pone.0214819.
Murgia, M., Prpic, V., O, J., McCullagh, P., Santoro, I., Galmonte, A., Agostini, T., 2017. Modality and perceptual-motor experience influence the detection of temporal deviations in tap dance sequences. Frontiers in Psychology 8, 1340. https://doi.org/10.3389/fpsyg.2017.01340.
Nixon, P.D., Passingham, R.E., 2001. Predicting sensory events: The role of the cerebellum in motor learning. Experimental Brain Research 138 (2), 251–257. https://doi.org/10.1007/s002210100702.
Oestreich, L.K.L., Whitford, T.J., Garrido, M.I., 2018. prediction of speech sounds is facilitated by a functional fronto-temporal network. Frontiers in Neural Circuits 12, 43. https://doi.org/10.3389/fncir.2018.00043.
Oldfield, R.C., 1971. The assessment and analysis of handedness: The Edinburgh Inventory. Neuropsychologica 9 (1), 97–113. https://doi.org/10.1016/0028-3932(71)90067-4.
Perrachione, T.K., Ghosh, S.S., 2013. Optimized design and analysis of sparse-sampling fMRI experiments. Frontiers in Neuroscience 7, 55. https://doi.org/10.3389/fnins.2013.00055.
Pfordresher, P.Q., 2006. Coordination of perception and action in music performance. Advances in Cognitive Psychology 2, 183–198. https://doi.org/10.2478/v10053-008-0054-8.
Pizzera, A., Hohmann, T., Streese, L., Habbig, A., Raab, M., 2017. Long-term effects of acoustic reafference training (ART). European Journal of Sport Science 17 (10), 1279–1288. https://doi.org/10.1080/17461391.2017.1381767.
Poldrack, R.A., Mumford, J.A., Nichols, T.E., 2011. Handbook of Functional MRI Data Analysis. A Practical Approach to Medical Image Processing. Cambridge University Press. https://doi.org/10.1017/CBO9780511895029.
Popa, L.S., Ebner, T.J., 2019. Cerebellum, predictions and errors. Frontiers in Cellular Neuroscience 12, 524. https://doi.org/10.3389/fncel.2018.00524.
Posner, M.I., 2012. Imaging attention networks. NeuroImage 61 (2), 450–456. https://doi.org/10.1016/j.neuroimage.2011.12.040.
Posner, M.I., Rothbart, M.K., 2007. Research on attention networks as a model for the integration of psychological science. Annual Review of Psychology 58, 1–23. https://doi.org/10.1146/annurev.psych.58.110405.085516.
Repp, B.H., 1999. Effects of auditory feedback deprivation on expressive piano performance. Music Perception 16 (4), 409–438. https://doi.org/10.2307/40285802.
Saunders, J.A., Knill, D.C., 2003. Humans use continuous visual feedback from the hand to control fast reaching movements. Experimental Brain Research 152 (3), 341–352. https://doi.org/10.1007/s00221-003-1525-2.
Saunders, J.A., Knill, D.C., 2005. Humans use continuous visual feedback from the hand to control both the direction and distance of pointing movements. Experimental Brain Research 162 (4), 458–473. https://doi.org/10.1007/s00221-004-2064-1.
Saygin, A.P., Wilson, S.M., Hagler, D.J., Bates, E., Sereno, M.I., 2004. Point-light biological motion perception activates human premotor cortex. Journal of Neuroscience 24 (27), 6181–6188. https://doi.org/10.1523/JNEUROSCI.0504-04.2004.
Schaffert, N., Janzen, T.B., Mattes, K., Thaut, M.H., 2019. A review on the relationship between sound and movement in sports and rehabilitation. Frontiers in Psychology 10, 244. https://doi.org/10.3389/fpsyg.2019.00244.
Schepers, M., Giuberti, M., Bellusci, G., 2018. Xsens MVN: Consistent Tracking of Human Motion Using Inertial Sensing. XSens Technologies 1–8. https://doi.org/10.13140/RG.2.2.22099.07205.
Schubotz, R.I., 2007. Prediction of external events with our motor system: Towards a new framework. Trends in Cognitive Sciences 11 (5), 211–218. https://doi.org/10.1016/j.tics.2007.02.006.
Schurz, M., Radua, J., Aichhorn, M., Richlan, F., Perner, J., 2014. Fractionating theory of mind: A meta-analysis of functional brain imaging studies. Neuroscience and Biobehavioral Reviews 42, 9–34. https://doi.org/10.1016/j.neubiorev.2014.01.009.
Senna, I., Cuturi, L.F., Gori, M., Ernst, M.O., Cappagli, G., 2021. Editorial: Spatial and temporal perception in sensory deprivation. Frontiers in Neuroscience 15, 671836. https://doi.org/10.3389/fnins.2021.671836.
Shadmehr, R., Smith, M.A., Krakauer, J.W., 2010. Error correction, sensory prediction, and adaptation in motor control. Annual Review of Neuroscience 33, 89–108. https://doi.org/10.1146/annurev-neuro-060909-153135.
Shima, K., Tanji, J., 2000. Neuronal activity in the supplementary and presupplementary motor areas for temporal organization of multiple movements. Journal of Neurophysiology 84 (4), 2148–2160. https://doi.org/10.1152/jn.2000.84.4.2148.
Smith, S.M., Jenkinson, M., Woolrich, M.W., Beckmann, C.F., Behrens, T.E.J., Johansen-Berg, H., Bannister, P.R., Luca, M.de, Drobnjak, I., Flitney, D.E., Niazy, R.K., Saunders, J., Vickers, J., Zhang, Y., Stefano, N.de, Brady, J.M., Matthews, P.M, 2004. Advances in functional and structural MR image analysis and implementation as FSL. NeuroImage 23 (Suppl 1), S208–S219. https://doi.org/10.1016/j.neuroimage.2004.07.051.
Stadler, W., Schubotz, R.I., von Cramon, D.Y., Springer, A., Graf, M., Prinz, W., 2011. Predicting and memorizing observed action: Differential premotor cortex involvement. Human Brain Mapping 32 (5), 677–687. https://doi.org/10.1002/hbm.20949.
Stokes, M., Thompson, R., Cusack, R., Duncan, J., 2009. Top-down activation of shape-specific population codes in visual cortex during mental imagery. The Journal of Neuroscience 29 (5), 1565–1572. https://doi.org/10.1523/JNEUROSCI.4657-08.2009.
Tal, I., Large, E.W., Rabinovitch, E., Wei, Y., Schroeder, C.E., Poeppel, D., Zion Golumbic, E., 2017. Neural entrainment to the beat: the "missing-pulse" phenomenon. The Journal of Neuroscience 37 (26), 6331–6341. https://doi.org/10.1523/JNEUROSCI.2500-16.2017.
Tivadar, R.I., Knight, R.T., Tzovara, A., 2021. Automatic sensory predictions: A review of predictive mechanisms in the brain and their link to conscious processing. Frontiers in Human Neuroscience 15, 702520. https://doi.org/10.3389/fnhum.2021.702520.
Wang, P., Jiang, Y., Hoptman, M.J., Li, Y., Cao, Q., Shah, P., Klugah-Brown, B., Biswal, B. B., 2023. Structural-functional connectivity deficits of callosal-white matter-cortical circuits in schizophrenia. Psychiatry Research 330, 115559. https://doi.org/10.1016/j.psychres.2023.115559.
Waszak, F., Cardoso-Leite, P., Hughes, G., 2012. Action effect anticipation: Neurophysiological basis and functional consequences. Neuroscience and Biobehavioral Reviews 36 (2), 943–959. https://doi.org/10.1016/j.neubiorev.2011.11.004.

Williams, A.M., Ford, P.R., Eccles, D.W., Ward, P., 2011. Perceptual-cognitive expertise in sport and its acquisition: Implications for applied cognitive psychology. Applied Cognitive Psychology 25 (3), 432–442. https://doi.org/10.1002/acp.1710.
Worsley, K., Friston, K., 1995. Analysis of fMRI time-series revisited-again. NeuroImage 2 (3), 173–181. https://doi.org/10.1006/nimg.1995.1023.
Zatorre, R.J., Halpern, A.R., 2005. Mental concerts: Musical imagery and auditory cortex. Neuron 47 (1), 9–12. https://doi.org/10.1016/j.neuron.2005.06.013.
Zhang, L., Qiu, F., Zhu, H., Xiang, M., Zhou, L., 2019. Neural Efficiency and Acquired Motor Skills: An fMRI Study of Expert Athletes. Frontiers in Psychology 10, 2752. https://doi.org/10.3389/fpsyg.2019.02752.